Università degli Studi di Padova

DIPARTIMENTO DI INGEGNERIA INDUSTRIALE
Corso di Laurea Magistrale in Ingegneria Meccanica

Direct Numerical Simulation of Non Premixed Jet Flames

Simulazione Numerica Diretta della Combustione Non Premiscelata in Getti

Candidato:
Ottavia Guidi
Matricola 1105029

Relatore:
Prof. Francesco Picano

Correlatore:
Federico Dalla Barba

Anno Accademico 2016–2017

Contents

Chapter 1

Introduction

Flame propagation is a central problem in most practical combustion systems, usually used in power generation and transport applications. Combustion is certainly one branch of science that affects almost every aspect of human activities. Hence it is crucial to improve combustion devices in industrial applications in order to reduce environmental pollution through a fundamental understanding of the involved phenomena.
Several combustion systems, as automotive and aeronautical engines, have a direct injection of liquid fuel. In this case, before chemical reactions may occur it is necessary that fuel evaporates and then mixes with the oxygen. This process is characterized by multi-scale phenomena such as turbulent velocity fluctuations, chemical reactions and temperature variations. These complex dynamics strongly reduce the possibility to simulate real systems accounting for all these effects.
Hence there is a continuing need for reliable and accurate models in combustion which can reproduce the main experimental flames in the simplest way as possible. In particular, present combustion models strongly differ as a function of the combustion regimes: premixed or non-premixed. In the former reactants are molecularly mixed and can burn, in the latter they need to mix first and then burn, e.g. liquid fuel combustion. From a phenomenological point of view, the main difference is that premixed systems show own flame propagation speed, while the others do not and are 'mixing' controlled. For this reason, in order to achieve a stable non-premixed flame without lift-off and blow-up it is necessary to have a small region with a propagating premixed flame. This twofold behavior is critical for modeling and need to be better characterized and understood.
Recently, the increased computer capabilities allow to simulate combustion problems in reduced scale, but taking into account the whole multiscale nature of the process. This numerical technique is called Direct Numerical

Simulation (DNS) and directly solves Navier-Stokes equations without using any turbulence model and so it can be considered the most accurate technique available, but requires huge computational resources. This technique can be seen as a virtual (small-scale) experiment that can be used to understand the physics of turbulent combustion in order to provide useful data for modeling purposes.
In this context, the present thesis concerns a turbulent non-premixed combustion of an heptane jet in co-flowing hot air focusing on the physical process of combustion. Heptane can be used either in liquid or gaseous state allowing to study both liquid and gas fuel combustion. However, in the present work only gaseous heptane in air is considered as a first step of a longer project which will consider heptane spray turbulent combustion.
Simulations have been carried out using an existing 3D parallel code: CYCLON, that has been modified to introduce heptane combustion process. A global scheme has been implemented and tested against available data. Then three simulations have been performed, two in laminar axysimmetric (2D) conditions and the latter in a turbulent 3D case. All the simulations concern a coaxial non-premixed autoingnited jet with different inflow velocities.
A characterization of the local combustion regimes is accomplished in all configurations. In all flames we note that premixed combustion is necessary to ignite and stabilize the whole flame although the large part of the combustion occurs in the non premixed regime.
Present results indicate that models based on the non-premixed framework will properly work for the large part of these flames, but will be probably inaccurate to predict flame stabilization which occurs in the premixed regime. From the prospective point of view it will be intresting to note how much these results change using liquid heptane sprays.

Chapter 2

Combustion's Physics and Chemistry

2.1 A Definition of Combustion

Combustion and its control are essential to the existence on this planet. Pratical combustion problems can be divided into five major categories:

- Energy producton and combustion device (combustion energy is mainly used to generate heat and power despite the alternative energy sources aviable such as geotermal, nuclear, solar and hydroelectric).
- Pollution production (carbon monoxide, SO_x, NO_x and unburned hydrocabons that are related to human health).
- Safty (the understanding of the dynamic fire propagation is essential for the prevention of blazes and exposions).
- Fuels (needed for combustion to take place).
- Defence and space (high energy munitions and propellants).

Moreover it is an interdisciprinary subject and affects thermodynamics, chemical kinetics, fluid mechanics and transport phenomea.

Combustion can be difined *a rapid oxidation generating both light and heat, or only heat* and it is the study of chemically reacting flows with rapid, highly exotermic reactions.
The terms oxidation in this definition emphasizes the importance of chemical reactions to combustion: they intrinsically imply the traformation of energy stored in chemical bonds to heat and combustion products.

At global level a combustion system consists of two reactants: fuel and oxidizer that must be mixed together at the molecular level before reaction can take place.
Combustion phenomena can be divided in two different categories based on the state of mixedness of the reactants. This classification of combustion can be consider the most important one and the two categories are *premixed* and *non-premixed* or *diffusional* combustion.
In a premixed combustion system the reactants are already well mixed before reaction is initiated while in a non-premixed system the reatctants, initially separeted, are brought together through both the molecular process of diffusion and, in this case, the convective motion due to the turbulence.
(It is important to recognize that, by calling a non-premixed system diffusional, doesn't imply a premixed system is nondiffusional).
In the present work a non-premixed combustion is being analised so it intended to underline the word "diffusion" because it indicates the need to bring the reactants together via this transport mechanism that is essential in mixing at the molecular level.
However in pratical device, both type of combustion may be present in various degrees.

Combustion can also be characterized by the nature of the flow in laminar or turbulent.
While in laminar flow distinct streamline exist for the bulk, in a turbulent flow quantities that randomly fluctuate in time can be found in space at any point.
Turbulence has a particularly influence on non-premixed combustion because it generally facilitates the mixing process of the reactants.
For this reason, turbulence is expected to increase the burning intensity both enhancing the mixing of reactants and the transport of heat and increasing the total flame surface area by wrinkling.
On the other hand if turbulent eddies are excessively intense, they can also cause a local flame extinction but at the same time chemical heat released in the combustion reaction try to preserve the structure of a turbulent flow.

From a chemical point of view, thermodynamics is an essential instrument to understand the equilibrium states of reacting multicomponent systems both thermal and chemical, in fact global performance parametres such as heat and power output can be estimated by assuming thermodynamic equilibrium of the combustion products.
Fuels can be classified according to their physical states under normal conditions and their rapresentive components are usual hydrogen, carbon monox-

ide and hydrocarbons; For most of the pratical combustion devices they react only with the oxygen but air, for pratical calculations is consider to consist of 21 percent oxygen and 79 percent nitrogen(which is basically inert) in molar conentration: $Air = 0.21O_2 + 0.79N_2$.
Combustion intensity between fuel and oxidizer depends on their relative concentrations: when their concentration ratio is chemically correct, reactants can be totally consumed, the burning mode is calling *stoichiometric reaction* and the combustion intensity is high.

Stoichiometric Reaction The stoichiometric quantity of oxidizer is the exactly amount needed to completely burn a quantity of fuel.
When the quantity is not just that amount needed the mixture can be defined lean if more than a stoichiometric quantity of oxidizer is supplied or rich if the oxidizer quantity is less than the stoichiometric ones.
Assuming that fuel reacts to form an ideal set of products, the stoichiometric oxidizer-fuel ratio can be determined by writing simple atoms balance.

$$(F/A)_{stioc} = \big(\frac{m_{fuel}}{m_{air}}\big)_{stoic} \tag{2.1}$$

It is commonly used also the *equivalent ratio* Φ to indicate quantitatively if the fuel-oxidizer mixture in lean, rich or stoichiometric:

$$\Phi = \frac{(F/A)_{stoic}}{(F/A)} \tag{2.2}$$

From this definition for $\Phi > 1$ the mixture is rich, $\Phi = 1$ stoichiometric mixture and for $\Phi < 1$ it is lean.

2.2 Chemical Kinetics

2.2.1 Reaction Rate

Chemical kinetics is a specialized field of physical chemistry which studies elementary reactions and their rates. Understanding chemical processes is essential to this study: in many combustion precesses chemical reaction rate controls the rate of combustion, ignition and flame extinction.
The overall reaction of a mole of fuel with A moles of oxidizer to form B

moles of products can be expressed by a global reaction mechanisms:

$$F + AOx \longrightarrow BPr \tag{2.3}$$

Progressively the rate at which the fuel is consumed can be expressed as a function both of the reactant concentrations according with the *law of mass action* and of the temperature accoring with *the Arrhenius law*:

$$\omega = k(T)[F]^m[Ox]^n e^{\frac{-Ea}{RT}} \tag{2.4}$$

Where ω is the rate constant, k is the global rate coefficient, m and n are exponents related to the raction order, Ea is the activation energy, R is the universe gas constant and T is the absolute temperature.
Before going on it intended to specify that the use of a global reaction to express the chemistry in a problem is unrealistic because in reality A oxidizer molecules can't simultaneously collide with a single fuel molecule to form B product molecules; in a real combustion process many sequential reactions can occur, however the global reaction approach may be useful in solving the present problem which isn't intrested in a detailed chemical comprehension. The previous rate expression can well satisfy the requirements of acceptable predictions of the variaton of burning velocity with stochiometry and turbulence.
In the case treated in the present thesis, the fuel(hepane), is a paraffin.
Giving an overview of praffins' oxidation process it can be said that it's characterized by three sequential macroprocesses:

- The fuel molecule is attacked by oxigen, atoms of hydrogen breaks dowm and oleofins are formed.
- The oleofins oxidize to CO and H_2 that is converted to water.
- The CO burns forming CO_2 and hydrogen.

The equations for the global reaction and the reaction rate in this case must be modify as follows:

$$C_xH_y + (\frac{x+y}{4})O_2 \longrightarrow xCO_2 + (\frac{y}{2})H_2O \tag{2.5}$$

$$\omega = k(T)[C_xH_y]^m[O_2]^n e^{\frac{-Ea}{RT}} \tag{2.6}$$

Where the parameters *k,Ea,R,m* and n are experimental data that are going to be seen in chapter5.

2.2.2 The Law of Mass Action

For a single, foward chemical reaction that can be represented by

$$\sum_{i=1}^{N} \nu_i^{'} M_i \longrightarrow \sum_{i=1}^{N} \nu_i^{''} M_i, \tag{2.7}$$

the rate of change in molar concentration c_i of the i-species, $\omega_i = \frac{dc_i}{dt}$, is uniquely related to the rate of the j-species and since it is species indipendent, it can be define as the reaction rate of the (2.7).
Then the phenomenological mass action's law states that ω is proportional to the product of the concentrations of the reactants

$$\omega = k(T)\Pi_{i=1}^{N} c_i^{\nu_i^{'}} \tag{2.8}$$

where $k(T)$ is a proportionally factor primarily a function of temperature.
This equation has been detracted being based on a molecular point of view which shows that the reaction rate is proportional to the collision frequncy.
Taking as an example the ganeral elementary reaction (2.6), the reaction rate is given by:

$$\omega = k[F][O_x] \tag{2.9}$$

Now let's consider a chemical system of N species reacting through M reactions:

$$\sum_{i=1}^{N} \nu_{im}^{'} \Theta_i \longrightarrow \sum_{i=1}^{N} \nu_{im}^{'} \Theta_i for \quad m = 1...M \tag{2.10}$$

where Θ_i is a symbol for species i and $\nu_{im}^{'}, \nu_{im}^{''}$ are the molar stoichiometric coefficients of species i in reaction m.
In this case it is important also to define a mass reaction rate for species i, $\dot{\omega}_i$, that is the sum of rates $\dot{\omega}_{im}$ produced by all M reactions:

$$\dot{\omega}_m = \sum_{m=1}^{M} \dot{\omega}_{im} = W_m \sum_{m=1}^{M} \nu_{im}\omega_m \tag{2.11}$$

where ω_m is the rate of progress of reaction m.
In addiction if there is a backward reaction associated with every forward reaction it have to be write:

$$\sum_{i=1}^{N} \nu_{im}^{'}\Theta_i \rightleftharpoons \sum_{i=1}^{N} \nu_{im}^{''}\Theta_i \quad m = 1, ..., M \tag{2.12}$$

$$\omega_m = k_{m,f}\Pi_{i=1}^{N} c_i^{\nu_{im}^{'}} - k_{m,b}\Pi_{i=1}^{N} c_i^{\nu_{im}^{''}} \quad m = 1, ...M \tag{2.13}$$

$$\omega_i = \sum_{m=1}^{M} (\nu_{im}^{''} - \nu_{im}^{'})\omega_m \tag{2.14}$$

Obviusly if the M elementary steps are identified and their associated reaction rate constants are known, the rates of production and destruction of any species can be precisely determinated.
However this is frequently difficoult and even if the steps are known, solving a combustion flow field by including all reaction is an extremely taxing task.

2.2.3 The Arrhenius Law

The specific reaction rate constant gives the functional dependence of raction rate on temperature; if the activation energy of the reaction is a constant and also the universal gas constant has a constant value it is conveniet to define a new quantity T_a:

$$T_a = \frac{E_a}{R} \tag{2.15}$$

and call it the activation temperature of the raction. So the Arrhenius equation can be modified:

$$\frac{dln\omega(T)}{dT} = \frac{E_a}{RT^2} \tag{2.16}$$

$$\omega(T) = Ae^{\frac{-T_a}{T}} \tag{2.17}$$

For a constant value of the pre-exponential factor it can be made a plot of $ln\omega(T)$ versus $1/T$ which exibits a linear relationship(Fig 2.1).

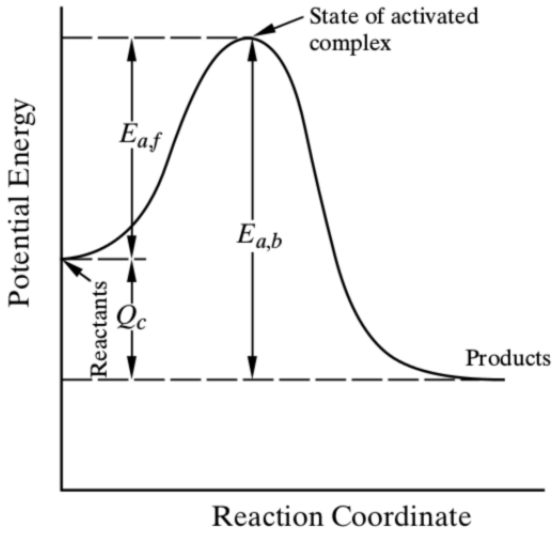

Figure 2.1: Potential energy diagram showing the concept of activation of a chemical reaction

Expressing $A = A(T) = BT^{\alpha}$ another modified Arrhenius equation can be introduced:

$$\omega(T) = BT^{\alpha}e^{\frac{-E_a}{RT}} \tag{2.18}$$

where B is a constant and α is a temperature exponent.
With such kinetic rate expressions, it is essential to specify the temperature range over which the numerical fitting of the experimental data is performed to determin the Arrhenius' parameters.

For a one-step global raction a description of the kinetic rate expression is quite difficoult and usually the curve shown in the graphic need to be approximated by a series of segments, each of which has its own kinetic constant of

frequancy factor, temperature exponent and activation energy.
A numerical fitting of this experimental data constitutes an effort to force a detailed reaction mechanism to conform to a simplified scheme.
Because off the activation energy assumes an important role, it is intended to open a short parenthesis explaining on what it consists.

The Activation Energy The activation energy represent the minimum energy that the molecules must have for the reaction to take place.
In fact the sensivity of a chemical reaction to the variations of temperature depends on the activation energy: the larger the activaton energy, the more sensitive is the reaction.
The largeness of the activaton energy is measured by the Arrhenius number defined as:

$$Ar = \frac{E_a}{RT_{max}} \tag{2.19}$$

where T_{max} is a reference maximum temperature in the flow-filed.
Ar can be interpred as a measure of the ratio of the activation energy to the maximum thermal energy in the flow.

2.2.4 Global Chemistry for Heptane/Octane Air Flames

The simpliest overall reaction representing the oxidation of a conventional hydrocarbon fuel is:

$$Fuel + n_1 O_2 \longrightarrow n_2 CO_2 + n_3 H_2 O \tag{2.20}$$

where n_i are determined by the choice of fuel.
The global reaction is often a convenient way of approximating the effects of the many elementary reactions which actually occurs and its rate must therefore represent an appropriate average of all of the individual reaction rates involved. The rate expression of a single reaction can be expressed

$$\omega = AT^n exp(-Ea/RT)[Fuel]^a [Oxidized]^b \tag{2.21}$$

In the present work it has been considered the oxidizer to be molecular oxigen and the hydrocarbon fuels studied are n-heptane and n-octane.

The most common assumption that can be found in the combustion literature for their concentration exponents is that the rate expression is first order in both fuel and oxidizer, however this assumption leads to serious errors in computed flame speeds, particularly for rich mixtures; than significant improvements in predicted flame speeds has be obtained with different choices for the concentration exponents a and b because it has been demonstrated that the flame speed depends strongly on the fuel concentration exponent a for rich mixtures and on the oxygen concentration exponent b for lean mixtures.
The best agreement between computed and experimental results for octane and heptan fuels has been obtained experimentally by Westbrook and Dryer and are well exposed in their article "Simplified Reaction Mechanisms for the Oxidation of Hydrocarbon Fuels in Flames". For the n-octane the best rate expression found is

$$\omega = 4.6 \cdot 10^{11} exp(-30/RT)[C_8H_{18}]^{0.25}[O_2]^{1.5} \tag{2.22}$$

while for the n-heptane it is the subsequent:

$$\omega = 5.1 \cdot 10^{11} exp(-30/RT)[C_7H_{16}]^{0.25}[O_2]^{1.5} \tag{2.23}$$

2.3 Thermochemistry

2.3.1 First and Second Law

The energy conservation is the foundamental principle embodied in the first law.
This law states that for a fixed mass, in a closed system, if the heat δQ is added to the system in an infinitesimal process, it is used to increase its internal energy δE and to perform a certain amount of work δW

$$\delta Q = dE + \delta W \tag{2.24}$$

Where E is a propriety of the system and the work can be considered done only by volume change caused by the pressure since the thermodynamics of a equilibrium chemical system is considered.

$$\delta Q = dE + pV \tag{2.25}$$

Alternativly a fixed control volume can be considered, in the control volume

the fluid may flow across the boundaries that don't move eliminating the need to consider change in kinetic and potential energies.
Fluid proprietis are considered uniform and not variable in time at each point within the control volume and there is only a one inlet and one exit stream. Under the previous hypotheses the equation becomes:

$$\dot{Q}_{cv} - \dot{W}_{cv} = \dot{m}e_o - \dot{m}e_i + \dot{m}(p_o v_o - p_i v_i) \tag{2.26}$$

where the subscripts cv, o and i denote the control volume and the outlet and inlet respectivitly.
The second law of the thermodynamics affirm that there exist a quantity S called entropy such that:

$$T\delta S \geq \delta Q \tag{2.27}$$

where T is the temperature and in all natural processes the inequality prevails.
From the second law it infers the concept of chemical equilibrium: considering a fixed volume, an adiabatic chemical reaction and fixed mass of reactants from products, as the reactions proceed temperature and pressure rise until a final equilibrium is reached.
The entropy of the product mixture can be calculated by summing the entropies of the product species and because off the conditions choosen for the control volume, the second law requires that the entropy changes internal to the system: $dS \geq 0$; it can be seen that the reaction will spontaneously take place since dS is positive.

2.3.2 Enthalpy

Enthalpy of Formation An absolute or standardized enthalpy can be defined for any species, it is the sum of the enthalpy of formation , h_f, which takes into account the energy associated with chemical bonds, and the sensible enthalpy change, Δh_s, associated with the temperature.

$$h_i(T) = h^o_{f,i}(T_{ref}) + \Delta h_{s,i}(T_{ref}) \tag{2.28}$$

where $h_i(T)$ is the absolute enthalpy at temperature T, $h^o_{f,i}(T_{ref})$ is the entalpy of formation at standard reference state and $\Delta h_{s,i}(T_{ref})$ is the sensible

enthalpy change in going from T_{ref} to T.
It is important to underline that is necessary to define a standard reference state(T_{ref},P^o) indetified by the supercript o.
The enthalpy of formation have a clear physical interpretation as the net change in enthalpy associated with breaking chemical bonds of the standard state elements.
The absolute enthalpy for unit mass can also be written in the following way:

$$h_i(T) = \int_{T_{ref}}^{T} c_p \, dT + h^o_{f,i}(T_{ref}) \tag{2.29}$$

Enthalpy of Vaporization The enthalpy of vaporization or the latent heat of vaporizaton, h_{fg}, is defined as the heat required in a constant pressure process to completely vaporize a unit mass of liquid at given temperature.

$$h_{fg}(T, P) \equiv h_{vapour}(T, P) - h_{liquid}(T, P) \tag{2.30}$$

where T and P are the sauration temperature and pressure, respectively.
This is a very important parametre in many combustion processes because a liquid fuel droplet must first vaporize before it can burn and so the liquid-vapour phase change is foundamental.
The latent heat of vaporization for various fuels at their normal boiling points are usually tabulated and at given saturation temperature and pressure, it can be used with Clasius-Clapeyron equation to estimate the pressure variation with temperature.

$$\frac{dP_{sat}}{P_{sat}} = \frac{h_{fg}}{R} \frac{dT_{sat}}{T^2_{sat}} \tag{2.31}$$

Enthalpy of Combustion The enthalpy of reaction can be defined knowing how to express the enthalpy for mixtures of both reactants and products, or detailing specifically with combustion reactions it can be defined the combustion enthalpy that is numerically equal to the reaction enthalpy but with opposite sign.
To define the combustion enthalpy, the combustion process is assumed to be complete: all of the fuel and the hydrogen are converted to CO_2 and H_2O.
For the products to exit at the same temperature of the reactants, heat must

be removed; the amount of heat removed can be related to the reactants and products absoute enthalpies according to the first law deducing the definition of enthalpy of combustion Δh_R:

$$\Delta h_R \equiv q_{cv} = h_{prod} - h_{reac} \tag{2.32}$$

It is important to underline that the value of the enthalpy of combustion depends on the temperature choosen for its evaluation.

2.3.3 Adiabatic Flame Temperaturare

Two different adiabatic flame temperatures can be defined, one for constant pressure combustion and one for constant volume.
The present work is intrested in the first one and so the costant pressure adiabatic flame is being treated.
When a fuel-air mixture burns adiabatically at constant pressure the absulute enthalpy of the reactants at the initial state is equal to the absolute enthalpy of the products at the final state.
According to the first law it can be write:

$$h_{reac}(T_i, P) = h_{prod}(T_{ad}, P) \tag{2.33}$$

This equation can also be graphically illustrated in Fig. 2.2.

2.4 Combustion Parametres

Combustion Efficiency In pratical combustion devices, after the chemical reaction it can be found both incomplete and complete combustion products.
Under lean operation conditions the amounts of incomplete combustion products are small while under fuel-rich operating conditions these amounts may become substantial.
For this reason it is useful to define the combustion efficiency.

$$\eta_c = \frac{h_{reac}(T) - h_{prod}(T)}{m_{fuel}Q} \tag{2.34}$$

where h_{reac} and h_{prod} are the formation enthalpies of reactant and products

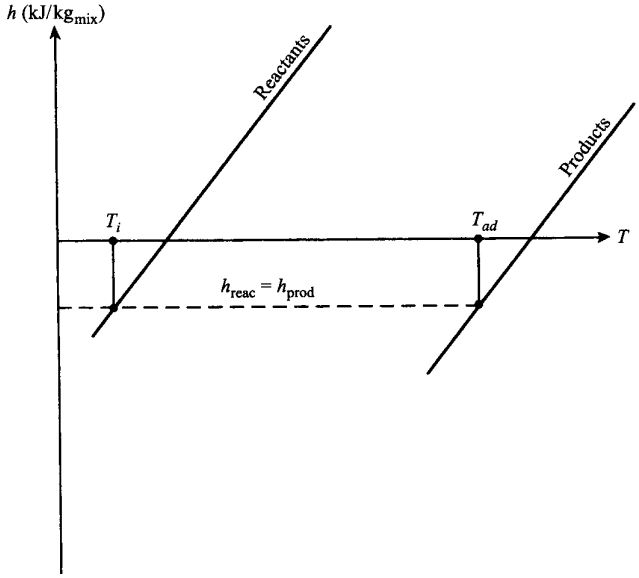

Figure 2.2: Constant pressure adiabatic flame on h-T

respectively at the given temperature T and the product $m_{fuel}Q$ rapresents the amount of energy which can be realeased by combustion.

Scalar Dissipation Rate The scalar dissipation rate characterized the inability of the mixture fraction to move through the gas phases and the intensity of the local diffusive tranfer.
It is defined as:

$$N = 2D|\nabla f|^2 \tag{2.35}$$

where D is the diffusion coefficient and f is the mixture fraction.

$$f = \frac{\nu Y_f - Y_o + Y_o^0}{\nu Y_f^0 + Y_o^0}$$

The scalar dissipation rate usually decreases with turbulent intensity because the turbulence makes the mixture fraction decrease facilitating the mixing between the fuel vapour and the surrounding gas flow.
However in region with low mixture fraction, higher tubulent intensity can lead to a larger scalar dissipation rate.

Flame Index In a combustion process, as alerady said, both premixed and non premixed combustion occur.
It is possible to quantify the contributions of each combustion type introducing the Flame Index defined as follows:

$$FI = \frac{1}{2}\big(1 + \frac{\nabla Y_F \nabla Y_O}{|\nabla Y_F \nabla Y_O|}\big) \tag{2.36}$$

A unity flame index indicates local premixed combustion while a $FI < 1$ indicates local non-premixed combustion.

Chapter 3

Flames

3.1 Laminar Flames

3.1.1 Laminar Premixed Flames

A laminar premixed flame is characterized by a structure which shows fresh gases and burnt gases separated by a thin reaction zone; the flame propagates toward the fresh gases beacuse of a local imbalance between the diffusion of heat and the chemical consuption and a strong temperature gradient can be observed. Thanks to this strong temperature gradient, fresh gases are preheated and start burning.
It can be said that in a laminar premixed flame , three regions can be identified:
- *The preheat zone* where the reaction starts: an increment of radical concentration, which are involved afterwards in the combustion, takes place and the heat released contibutes to the temperature growth.
- *The reaction zone* where the oxidation occurs with an high amount of heat release.
- *The recombination zone* where the most of the gases are completely burnt and the reaction can be considered come to an and.

Every laminar premixed flame has a propagation speed S_L which depends on various parameters like the temperatue of the fresh gases or the composition of the reagents. The flame speed is a central element in the combustion studies, for this reason multiple definitions can be found for it; the simpliest one is "the velocity at which the flame front moves with respect to the fresh gases" and can be expressed by the following equation:

$$S_L = -\frac{1}{\varrho Y_f} \int_{-\infty}^{\infty} \dot{\omega}_f dx \tag{3.1}$$

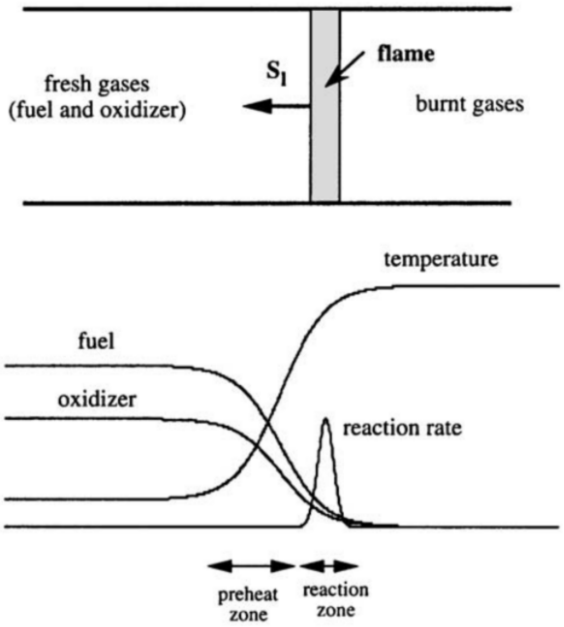

Figure 3.1: Structure of a laminar plane premixed flame

where ϱ, Y_f and ω_f are respectively the fuel density, mass fraction and reaction rate.
In a laminar flame also the concept of a flame thickness is introuced:

$$\delta = \frac{\lambda}{\varrho C_p S_L} \tag{3.2}$$

The flame thickness has a central role in solving many numerical combustion problems beacuse it controls the required mesh resolution.

3.1.2 Laminar Diffusion Flames

In a laminar diffusion flame, fuel and oxidizer are on both sides of the reaction zone where heat is released and the molecular diffusion of the reactants toward the reaction zone contols the burning rate; the amount of heat transported away from the reation zone is exactly balanced by the heat released by combustion.

The structure of a steady diffusion flame depends on ratios between the characteristic times of molecular diffusion and chemistry (where the molec-

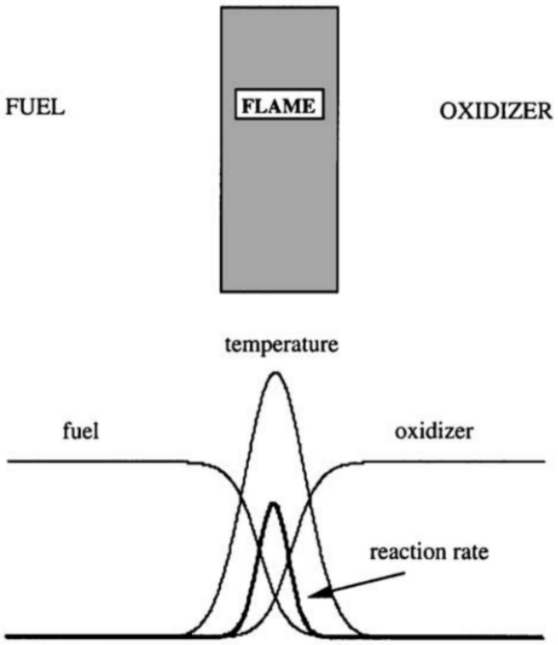

Figure 3.2: Structure of a laminar diffusion flame

ular diffusion is expressed using the Fick law), in fact the thickness of the reaction zone vary with this characteristic times.
In opposition with premixed flames, diffusion flames are mainly mixing controlled and their thickness is not constant but depends on the local flow propieties. In a diffusion flame also quenching can occur if the heat fluxes leaving the reaction are grater than the chemical heat production.
Its internal structure is usually discussed using the level of mixing between fuel and oxidizer defining the mixture fraction f which eveolves through the mixing layer from 0 (pure oxidizer) to 1 (pure fuel).

3.1.3 Partially Premixed Flames

In non premixed combustion some partial premixing of the reactants may exist before the reaction develops. This phenomenon of premixing between fuel oxidizer and than the burnt products leads to a stabilization mechanisms: as well as fuel and oxidizer are transported toward each other thanks to the diffusion and the convective motion, they become heated so that the reaction between them subsequently takes place rapidly arriving at the stochiometric

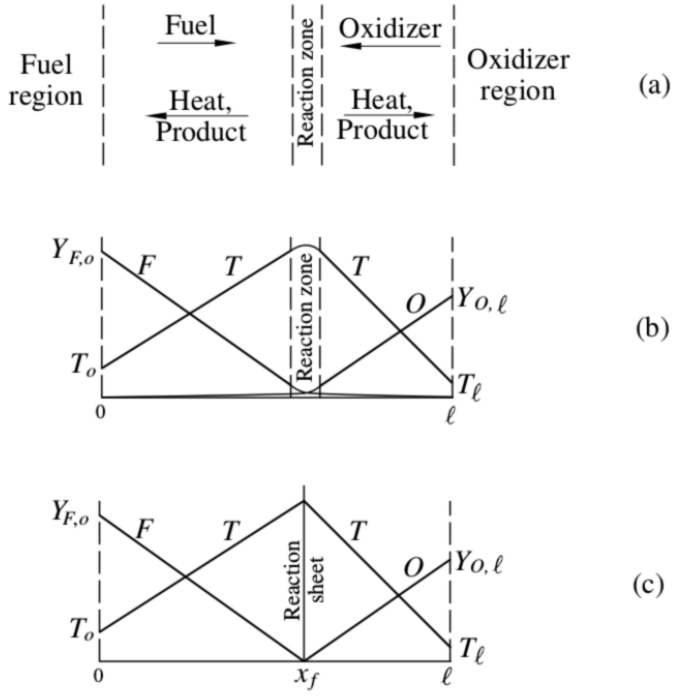

Figure 3.3: Real structure of a laminar non-premixed flame:(a)physical configuration; (b)temperature and concentration profiles with finite flame thickness; (c)temprature and concentration profiles with reaction sheet.

conditions.
Cobustion products and heat released are tranported away from the reaction zone in both directions but small amount of fuel and oxidizer remain in the reaction zone because a complete reaction cannot be accomplished until it occurs at a fine rate and in a finite thickness zone.
It is useful to assume that the reaction occurs infinitely fast and thereby it is confined to a reaction sheet.

Overall it can be said that in a real diffusional flame the structure consists of three zones with a reaction zone saparating a fuel-rich zone and a oxidizer-rich zone. This type of structure composed of two premixed flames an of a diffusion flame is called *triple fame* and it has been firstly experimentally observed by Philips(1965).

Tribrachial Flame In a triple flame, combustion starts in a region when fuel and oxidizer have benn mixing in a stoichiometric proportion. In the mix-

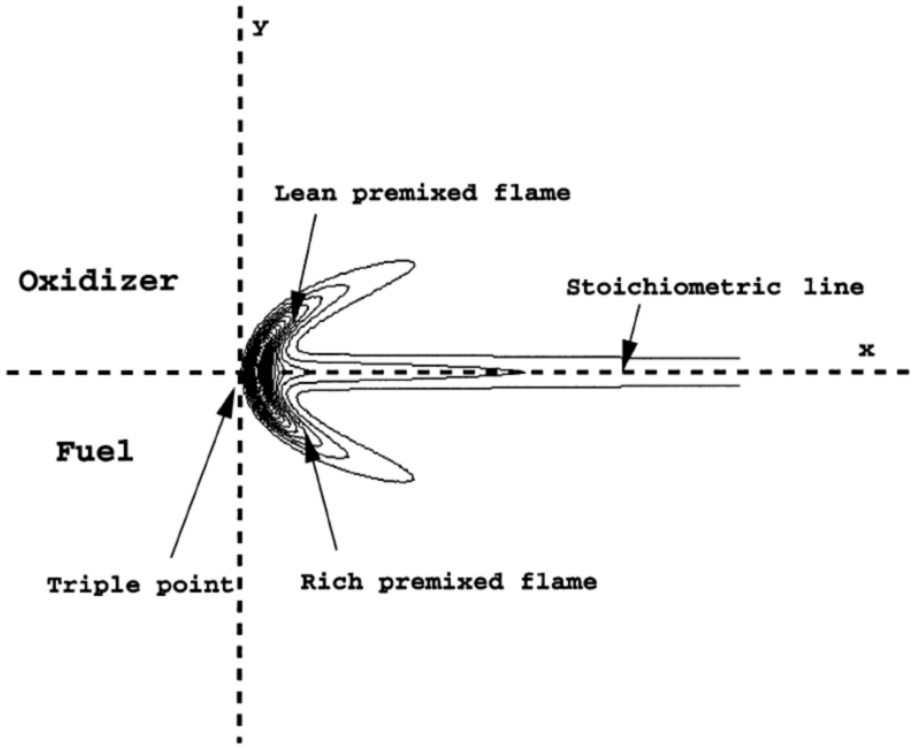

Figure 3.4: Scheme of the propagation of a triple flame.

ing layer configuration the stoichiometric premixed kernel tends to propagate evolving to a rich premixed flame in the direction of the fuel stream while a lean partially premixed flame develops on the air side; however the propagation velocities of this two premixed flames decrease when moving away from the stoichiometric conditions, for this reason the flames are curved.
The curvature of the partially premixed front and the heat released control the propagation speed of the triple flame. The effect of the heat release is to deflect the flow upstream making the speed of the tribrachial flame greater than the speed of the planar stoichiometic flame.

3.2 Turbulent Flames

3.2.1 Phenomenology of Turbulence

In pratical devices, turbulent flows are more frequently encountered than the lamiar ones; turbulent flow result when intabilities in a flow are stronger than

the viscous actions and the fluid velocity exibits random fluctuations at each point in the flow.
Turbulence is a stochastic, unsteady, random phenomena which change their proprieties in time.
The randomness make turbulence to be an extremely complex phenomena to analize, the mathematical description of a turbulent flow and the solution of the resulting governing conservation equations are very difficoult, in particoular compared to laminar flows.
In addiction, in turbulent flows experiments, there is not repeatability because they are high sensivity to their initial conditions: two flows characterized of infinitely small differences in initial conditions will evolve in a completely different way.
For this reason a statistical approach is being used to develop a satisfying description of turbulence.
A flow can also be defined turbulent when it assumes high values of the Reynolds number.
Osborne Reynolds found this parametre in a famous experiment in which transition from laminar to turbulent flow was visualized in a tube with a dye fluid streack; He recognized that the flow was completely identified by this single dimensionless number defined as follows:

$$Re = \frac{UL}{\nu} \tag{3.3}$$

where U is the characteristic velocity, L the characteristic length scale and ν the fluid kinematic viscosity.
It can be noted that it's defined as the ratio between the inertial foces and viscous ones.
This number is a key parametre for the turbulence phenomenology description; Typically, if its value is larger than 3000, the flow can be considered turbulent while if it is smaller than about 2000 it is considered a laminar flow.
(In the range between 2000 and 3000 the fluid is in a transient state).
A turbulent flow is also characterized by a velocity field which presents a non-zero vorticity, this vorticity field $\omega = \nabla \times u$ gives useful information in order to characterize turbulence defining each specific legth and velocity scales.
Because of this a turbulent flow is intrinsecally rotational.
In fact the velocity field generates "tubes" created by vorticity lines that are everywhere tangential to the istantaneous vorticity vector.
The evolution of the vorticity field can cause two types of pheomenology:

the vortex tilting and stretching; the first cosists in a vorticity stream's change due to a transversal velocity gradient, the second consists in a three-dimensional auto-amplification of the vortex due to a velocity gradient that is in the same direction of the vorticity field.
As a concequence of the vorticity, turbulence generates the so called eddies with a moltitude of scales: a number of smaller eddies may be imbedded in a larger eddy.
The rapid interwining of a wide range of legth scales and eddy sizes is a peculiarity of turbulent flows.
A measure of the range of scales present in a turbulent flow is expressed by the Reninolds number: the greter the Reinolds number, the greater the range of sizes from the larger eddy to the smallest.

The theory of Kolmogorov

Large eddies transfer kinetic energy to the smaller ones in a process called *energy cascade*(Fig. 3.5) until the kinetic energy is dissipatd by viscosity.
This process was first described by L.F.Richardson, in 1922, and furher invesigated by A.Kolmogorov.
Richardson gave only qualitative description of the turbulent flow behaviour

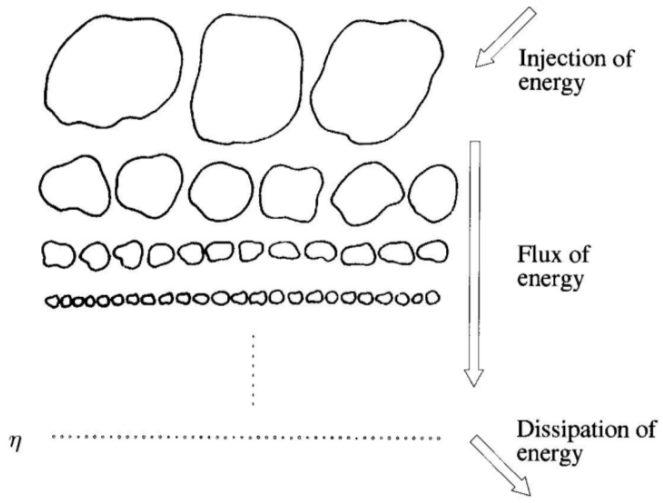

Figure 3.5: Energy Cascade. *"Big whorls have little whorls, which feed on their velocity, and little whorls have lesser whorls and so on to viscosity" Lewis F. Richardson.*

while Kolrmogorov, with his statistical analysis, found quantitative information about the dissipative eddies length.
Every eddy is characterized by a legth scale l, a characteristic velocity $u(l)$ and a time scale $\tau(l) \equiv \frac{l}{u(l)}$.
In a specific turbulent flow larger eddies have a length scale, l_0, which is of the same order of the flow scale L and a characteristic velocity, u_0, comparable to the flow's one U; so it can be said that $Re \equiv u_0 l_0/\nu$ is of the same order of the Reynolds number of the flow $Re = UL/\nu$ and at this legth the effect of viscosity is negligible.
The energy transfer from larger to smaller eddies continues until the Rynolds number of reciving eddies is low enough that the effect of viscosity become able to dissipate the kinetic energy.
The scale where viscosity effect become relevant, η, as previously said, is the Kolmogorv scale and its Reinolds number is one.
Kolmogorov scales parametres can be calculated through a dimensional analysis given ν and ϵ where ϵ is the rate of the energy dissipation that is imposed at the larger scales:

$$\eta \equiv \left(\frac{\nu^3}{\epsilon}\right)^{\frac{1}{4}} \tag{3.4}$$

$$u_\eta \equiv \left(\nu\epsilon\right)^{\frac{1}{4}} \tag{3.5}$$

$$\tau_\eta \equiv \left(\frac{\nu}{\epsilon}\right)^{\frac{1}{2}} \tag{3.6}$$

Than it can be demonstrate that the Reynolds number based on the Kolmogorov scales is unity ($Re_\eta = 1$):

$$\frac{\eta u_\eta}{\nu} \equiv 1 \tag{3.7}$$

This calculation process can be applicated because of the *First Kolmogorov Hypotheses* which concerns the *isotropy of the small-scale motions.*
Kolmogorov argued that, while the large eddies are anisotropic and affected by the boundary layer conditions, small-scale turbulent motions are statistically isotropic and universal: the directional biases of the large scales are lost in the chaotic scale-reduction process.
In addiction, by reason of the fact that the two dominant processes in the energy cascade are the transfer of energy and the viscous dissipation, the

kinematic viscosity and the rate of dissipation energy are the only parametres on which the statistically univesal state depends.
The previous considerations are well summarised in Kolmogorov's first similarity hypotheses.

Kolmogorov's first similarity hypothesis *In every turbulent flow at sufficiently high Reynolds number, the statistic of the small scale motions have a universal form that is uniquely determined by ν and ϵ.*

The smallest eddies dimension is really low compared with the integral legth scale, as a consequence it's clear that it exists a range of scales smaller than l_0 but greater than η. From this considerations the second similarity hypothses has been deduced.

Kolmogorov's second similarity hypotheses *In every turbulent flow at sufficient high Reynolds number, the statistic of the motion scale l in th range $l_0 \gg l \gg \eta$ has a universal form that is uniquely determined by ϵ, indipendent od ν.*

Eddy sizes, on a logaritmic scale, at high Reynolds number are shown in the subsequent figure with the various legthscale and range.

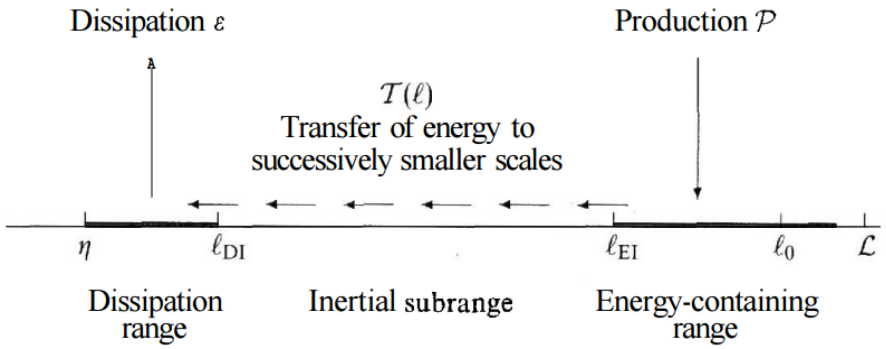

The lengthscale $l_{EI} \approx 1/6L$ has been introduced as the demarcation between the anisotropic large eddies ($l > l_{EI}$) and the isotropic small eddies ($l > l_{EI}$). This demarcation can also be defined as the division between the *energy-containing rage* $l_{EI} < l < L$ and the *universal equilibrium range*

$(l < l_{EI})$.
The lengthscale l_{DI} has been introduced to explain the split of the universal equilibrium range in two subranges: the *inertial subrange* $(l_{EI} > l > l_{DI})$ and the *dissipation range* $(l < l_{DI})$.
The inertial subrange includes the scales of the universal equilibrium range where inertial effects are predominant while the dissipation range includes the scales where molecoular dissipation is dominant.

3.2.2 Tubulent Premixed Flames

In a turbulent premixed flame, the laminar flame mode previously seen is replaced by a regime where turbulence and combustion interact. The first characteristic that distinguish this case form the laminar one is that the temporal scale of motion have to be compared with the chemical temporal scale. The interface that separates fresh and burnt gases, differently from the diffusion flame, is clear defined even if the turbulence is responsable for stresses and strains of the flame structure. The interaction between combustion and turbulence causes an increasing of convection and mixing between reactants and products along the flame front so that mass, momentum and heat release transport is enhanced.
The first description of turbulent premixed combustion is due to Damköler(1940), he has introduced the concept of wrinkling as the main mechanism which controls the turbulent flame stabilization. A turbulet flame speed has been defined as the velocity needed at the inlet, in a control volume to keep stationary a turbulent premixed flame inside this volume. It initially increases and this phenomenon has been explained by a simple phenomenological model which assumes that each point of the flame surface moves locally at the laminar flame speed; the increase of the turbulent flame speed S_T, compared with the laminar one is due to increase of the total flame area A_T, caused by wrinkling, with respect to the cross section A.

$$\frac{S_T}{S_L} = \frac{A_T}{A} \tag{3.8}$$

The ratio A_T/A is called *flame wrinkling*, it correspond to the ratio of the aviable flame surface area divided by its projection in the propagation direction and it increases with the Reynolds number. However the local Reynolds number and also the kinematic viscosity change according to temperature change form one side of the flame front to other; the Reynolds number, in fact, is smaller in burnt gases than in fresh gases and it can lead a relaminar-

ization. In addiction there is an acceleration of the flow through the flame front that modifies the turbulent flow which is also affected by velocity and density changes.
As mentioned, it is important to compare turbulence and chemical characteristic length and time scales with the aim to analyze premixed turbulent combustion regimes, to do that it has been introduced the Damköhler number:

$$Da = \frac{\tau_t}{\tau_c} \tag{3.9}$$

Where τ_c is the chemical time while τ_k the turbulent time.
For large values of the Damkȯhler number ($Da \gg 1$), the flame front is thin and its inner structure is not affected by turbulence motions which only wrinkle the flame surface. This regime where the turbulent motions are too slow to affect the flame structure is called *falmelet regime*.
Then, when the turbulent motions become relevant, the regime transition is described in term of Karlovitz number:

$$Ka = \frac{\tau_c}{\tau k} \tag{3.10}$$

- When $Ka < 1$ the regime is the *flamelet regime* but two suddivision may be proposed depending on the velocity ratio:
  - u'/S_L¡1: *wrinkled flame*, the laminar propagation is predominant and turbulence.combustion interations remain limited.
  - u'/S_L¿1: *wrinkled flame wih pockets*, larger structures become able to induce flame front interactions leading to pockets.

- $1 < Ka \leq 100$: *thickened wrinkled flame regime*, turbulent motions are able to affect and to thicknen the flame preheat zone but cannot modify the reaction zone that remains thin and close to a laminar zone.

- $Ka > 100$: *thickned flame regime* , preheat and reaction zones are strongly affected by turbulent motions.

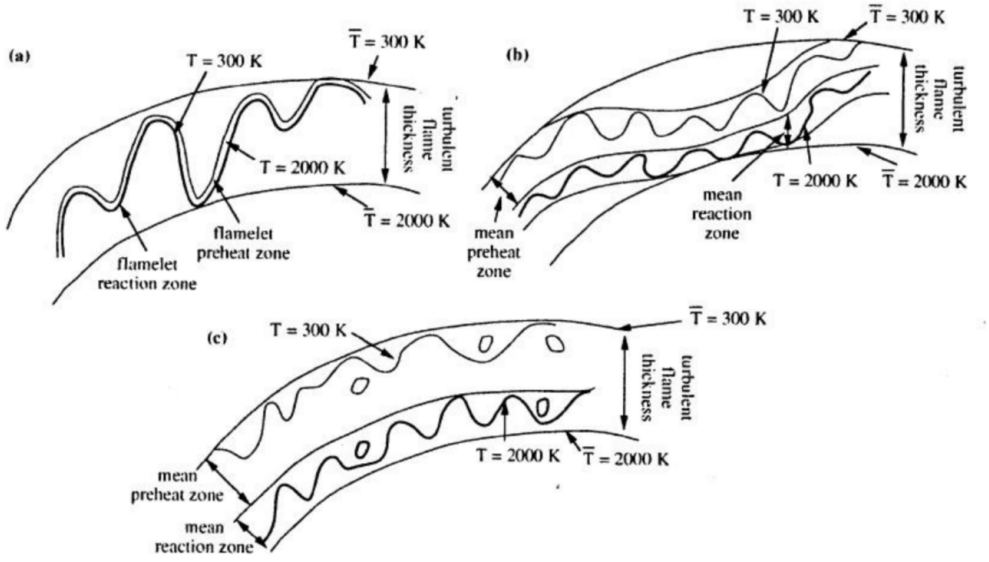

Figure 3.6: Turbulent premixed combustion regimes proposed by Borghi and Destriau: a) wrinkled flamelet (thin wrinkled flame), b)thickened-wrinkled flame, c) thickened flame.

3.2.3 Turbulent Non-premixed Flames

In non-premixed turbulent combustion the problem to find parameters with the aim to describe the flame is more difficult because diffusion flames don't propagates or exibit intrinsic characteristic speed; this property has consequences on the chemistry-turbulence interacion: without propagation speed a non premixed flame is unable to impose its own dynamics on the flowfield and it is more sensitive to turbulence. Diffusion flames are also more sentitive to stretch than turbulent premixed flames and are more likely to be quenched by turbulent fluctuations and flamlet assumptions can't be often justified.
In addicition the thickness of the flame depends on the aerodynamics which controls the thickness of the local mixing layers and no reference length scale can be easily identified.
It can be said that in a non-premixed turbuent flame, the reaction zone develops within a mean mixing zone whose thickness l_z is of the order of the turbulent integral scale l_t:

$$l_z \approx l_t \approx \left(\frac{k^{3/2}}{\epsilon}\right) \tag{3.11}$$

Turbulent small scale mixing depends both on velocity fluctuations and diffusion between the iso mixture fraction surfaces; when the Kolmogorov scale is of the order of the flame thickness the inner stucture of the raction zone may be modified by the turbulence.

The simpliest diffusion flame is a fuel jet decharging in ambient air, in this situation, oxidizer is provided to the flame zone through air entrainment and natural convection but after the ignition the incoming reactants must be continuously mixed and ignited by the hot products for combustion to continue. This process is called stabilization.
Predicting flame stabilization is also an unsolved problem, however triple flames also play a roe in stabilization mechanisms of turbulent non premixed combustion; such situations have been observed in direct numerical simulations (Domingo and Vervisch 143) and some experimental results (Muniz and Mungal, Schefer and Goix, Upatnieks et al.) show that triple flame-like structures are found in the stabilization reions of turbulent lifted flames. The instantaneous velocity measurements conducted by Muniz and Mungal in a lifted jet diffusion flame show that, despite a mean flow velocity larger than the flame speed, a triple-flame is able to sustain, the flame front is always located in a region where the instantaneous flow velocity is of the order of magnitude of the laminar flame speed and continuously moves to satisfy this

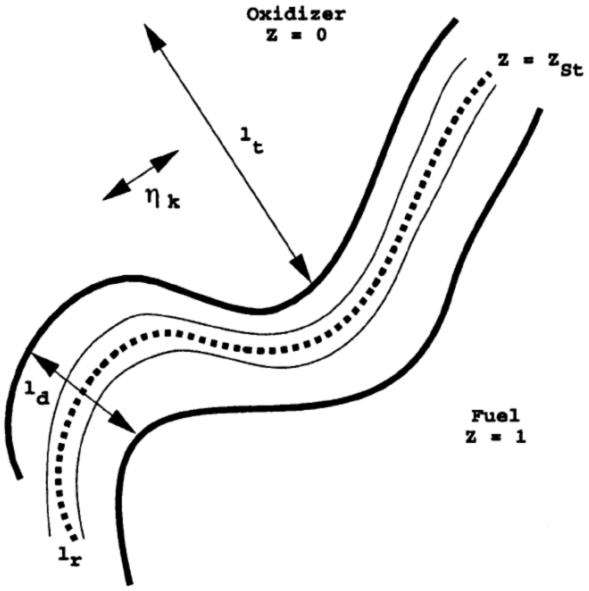

Figure 3.7: Scheme of a non premixed turbulent flame where Z is the mixture fraction, l_d the diffusive thickness, l_r the reaction zone thickness, l_t the turbulence integral length scale.

condition.
It is important to underline another phenomena able to influece the stabilization process: the auto-ignition. In fact, when one of the fuel or oxidizer streams is sufficiently hot, the flame stabilization may be ensured by auto-ignition processes inside the mixing layer, independently of the inlet speeds as shown in figure 3.8

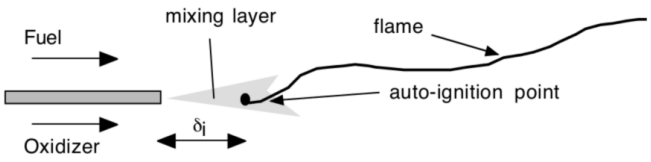

Figure 3.8: Turbulent non-premixed flame stabilization by auto-ignition processes.

Chapter 4

Flames Numerical Simulations

4.1 Computational Fluid Dynamics

Computational fluid dynamics(CFD) is a branch of fluid mechanics that uses numerical analysis and algorithmis to solve and analyze problems that involve fluid flows.
Computers are used to perform the calculations required to simulate the interaction of liquids and gases with surfaces defined by boundary conditions.
In a multy-phases turbulent reacting flow there are even bigger challenging issue which increase the complexity of the simulation leading to an extremely complex procedure and huge computational resources to solve the necessary equations.
The equations that have to be solved are the Navier-Stokes equations for turbulent reacting flows which, in most cases, have not an exact solution.
In order to numerically solve Navier-Stokes equations, several CFD techniques have been developed, they can be divided in three main groups that are characterized by different degrees of approximation:

- Direct Numerical Simulation(DNS): The time evolving Navier-Stokes equations are solved on a discrete mesh wihout using any turbulence model but resolving explicitly any scale of turbulent motion.
  Using this approach allows accurate simulations and datail descriptions of the flows' physics, however it require a considerable amount of computational capacity.

- Large Eddy Simulation(LES): In LES approach a sub-grid clousure model(e.g. Smagorinsky) is used to simulate the effects of the smaller

scales of turbulent motion while only larger scales are calculated explicity.
This type of simulation is based on the application of an opportune filtering operator to each fuid-dynamic field appearing in the Navier-Stokes equations.
Each variable can be decomposed into two parts: the filtered value and the field fluctuation ones(refered to its related filtered value). It can be write as follows:

$$\Phi = \tilde{\Phi} + \Phi^{'} \tag{4.1}$$

where $\tilde{\Phi}$ is the filtered value and $\Phi^{'}$ the fluctuation ones.
The filter operator cuts the stochastic fluctuatons of each field under a certain turbulent scale; with this cut LES can't capture the variations of flud dynamic fields under a certain frequency threshold but the computational resources required to solve the Navier-Stokes equations have been reduced drastically.

- Reynolds Averaged Navier-Stokes(RANS): In RANS approach a decomposition of the fluid dynamic fields appearing on the Navier-Stokes equations is carried out.
  Each variable is divided in a deterministic mean part defined by the ensamble averge taken over some set realizations, $< \Phi >$, and a stochastic contribution which rapresents the variable fluctuatons with respect to its mean value, $\Phi^{'}$.

$$\Phi =< \Phi > +\Phi^{'} \tag{4.2}$$

  RANS equations can be derived substituing Reynolds decomposition for every fluid dynamic fields in the Navie-tokes equations and then effectuating the ensemble average; the stochastic contribution is considered trough the "Reynolds stresses" represented by an unknown stress tensor.
  The estimation of this quatity requires some clousure models(e.g. $k-\epsilon$ *model* which make it possible to solve only the mean values of all quantities throwing the fluctuations away.

It can be said that, while in LES and RANS the use of some closure problem rules are essential, DNS is the most performant technique in terms of accuracy due to not requiring any clousure model.

DNS will be further discussed because in the present study a 3D DNS approach has been adopted to reproduce and investigate the dynamic of a turbulent reacting jet.

4.1.1 Direct Numerical Simulation

Initiated in the eighties, Direct Numerical Simulation is the most accurate numerical technique aviable to the purpouse of solving Navier-Stokes equations and it has changed radically the turbulent combustion studies and modeling. DNS, as previously underline, solves directly the full istantaneous equations considering explicitly all turbulent scales; Solving the flow equations without any turbulence model offers an interesting way to investigate flame-turbulence interaction.
In fact through DNS it is possible to predict all time variations of fluid dynamic fields exactly, describing reacting flows including multi-species transport, thermodynamics and chemistry.
One of the most critical issue of a simulation consists in the fluid domain discretization, all CFD methods requires space and time discretization but this step is more critical for DNS than for the other siulation technique because all scales of turbulent motion have to be resolved on the discrete mesh.
In the domain the all scales range from the Kolmogorov micro scale up to the length scale of larger eddies appears.
In order to obtain a full resolution of all the scales on the discrete mesh, the following requires:

$$n_s \Delta s \geq L \tag{4.3}$$

$$\Delta s \leq \eta \tag{4.4}$$

where n_s is the number of points along a given mesh direction with increments Δs and L is the length of the larger scale.
In the larger scale the eddies are carachterized by a velocity u_0 comparable to che flow velocity U so that its Reynolds number is $Re_0 = \frac{u_0 l_0}{\nu_0}$ comparable with the flow's Reynolds number.
Furthermore these larger eddies have energy of order u_0^2 and time scale $\tau_0 = \frac{l_0}{u_0}$ and the kinetic energy dissipation rate ϵ is determined by the transfer of energy from the lergest edies to the smallest ones; so the rate of energy transfer can be suppose to scale in the subsiquent way:

$$\epsilon \propto \frac{u_0^2}{\tau_0} \propto \frac{u_0^3}{l_0} \propto \frac{U^3}{L} \tag{4.5}$$

The energy transfer continues until the Reynolds number of reciving eddies is low enough that the dissipative effects of the viscosity become relevant and the kinetic energy is dissipated to heat; this happens at the Kolmogorov scale where the energy dissipation rate can be expressed as $\epsilon \equiv \frac{\nu^3}{\eta^4}$.
Moreover it is necessary for the advance of the solution in time to be accurate that a fluid particle moves only a fraction of the grid in a time step Δt:

$$\Delta t \leq \frac{\Delta s}{U}. \tag{4.6}$$

Considering the duration of a Direct Numerical Simulation, that express the time required by a fluid particle to move across the whole flow length scale L with a velocity U, equal to $t_{DNS} = L/U$, the number of the time steps can be estimated as follows:

$$n_t = \frac{t_{DNS}}{\Delta t}. \tag{4.7}$$

The previously considerations leads to the conclusion that the number of mesh points and time steps required by a DNS grow as a power law of the Reynolds number:

$$n_s^3 \geq Re^{\frac{9}{4}} \tag{4.8}$$

$$n_t \propto Re^{\frac{3}{4}} \tag{4.9}$$

The number of operations necessary to complete the simulation is proportional to the number of mesh points and the number of time steps which grow as a power low of Reynolds number; In fact it is possible to demonstrate that the number of operations necessary to solve a DND grows as $Re^{\frac{11}{4}} \approx Re^3$ .This make clear how the comptational cost of a DNS become extremely high and motivate the importance to develop efficients algorithms paying particoular attention to the optimization of computational resurces in order to follow the purpose of reducing them.

4.2 Combustion Phenomena

Cumbustion involves multiple species reacting through chemical reactions.
It is important to describe some quantities necessary to better understand the systematic mathematical formulation of the problem.
First, each species is characterized by its mass fraction:

$$Y_i = \frac{m_i}{m} for \quad i = 1, .., N \tag{4.10}$$

where N is the number of species in the reacting mixture, m_i is the mass of the species i present in a given volume and m is the total mass of the gas in the volume.
The mole fraction and the mole concentration are just as much common parameter to measure the conentrations of species:
The mole fraction X_i is the ratio of the number of moles of the i species in a specific volume to the total number of mols in the same volume; the molar concentration $[X_i]$ is the total number of moles of species i per unit volume.
There are also some important parameters related to the molecular transport of species and heat like the heat diffusion coefficient, λ, and the species diffusion coefficient, D_i, that are often connected together through the *Lewis Number* defined as follows:

$$Le_i = \frac{\lambda}{\varrho C_p D_i} \tag{4.11}$$

The Lewis number is a local quantity, it compares the diffusion speeds of heat and species i, and in most gases it can be considered a constant value because it changes very little from one point to another.
The *Prandlt number*, Pr:

$$Pr = \frac{\nu}{\lambda/(C_p)} = \frac{\mu C_p}{\lambda} \tag{4.12}$$

compares momentum and heat transport.
The *Schmidt number*, Sc_i, compares the momentum and the species heat diffusion:

$$Sc_i = \frac{\nu}{D_i} = PrLe_i \tag{4.13}$$

4.2.1 Burning

Before introducing the equations that have to be solved for the DNS, some aspect concerning the burning phenomena will be briefly discussed.
It is going to be considered the pure vapour that is dispersed into the surrounding carrier phase through the molecular diffusion driven by the vapour concentration gradient and the convective forces induced by external flow; in addiction to the external flow there is also the so-called Stefan flow which induces a forced convection.
This particoular flow consists of a mass transport process that occurs in a mixture of two or more chemical species caused by the removal or the production of one species at the interface: it induces a stream in the mixture which make the speies transport themselves by forced convection.
The diffusion process is speeded up when a burning process occurs thanks to the temperature grow.
Let's now consider the vaporized fuel trying to understand what happens across the flame sheet.
From the flame point of view two zones can be identified: the inner region where the diffusing species is the fuel vapour and the outer region where the diffusing species is the oxidizer.
Considering the oxidizer and fuel combine to stoichiometric proportions and the diffusion process menaged by the Fick's law, generally it can be write:

$$11 \quad kg \quad fuel + \nu \quad kg \quad oxidizer = (\nu + 1) \quad kg \quad products \tag{4.14}$$

In the inner region the fuel vapour concentration decreases until the flame sheet where $Y_f = 0$ and the fick's law is:

$$\dot{m}_f = -4\pi r^2 \frac{\varrho D}{1 - Y_f} \frac{dY_f}{dr}. \tag{4.15}$$

In the outer region the same consideration can be done for the oxidizer: at the flame sheet $Y_{ox} = 0$ and it can be write

$$\dot{m}_{ox} = -\nu \dot{m}_f \tag{4.16}$$

$$\dot{m}_{pr} = (\nu + 1)\dot{m}_f \tag{4.17}$$

$$\dot{m}_f = 4\pi r^2 \frac{\varrho D}{\nu + Y_{ox}} \frac{dY_{ox}}{dr} \tag{4.18}$$

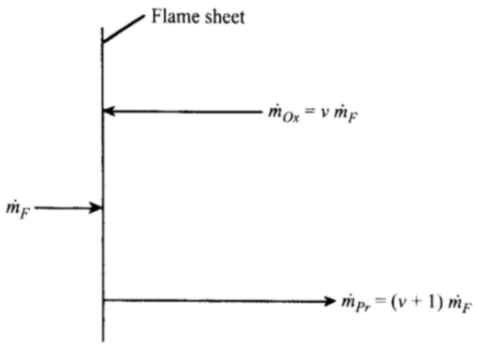

Figure 4.1: Mass flow relationships at flame sheet

Considering for example a single direction x in the inner region the combustion product mass fraction can be expressed as

$$Y_{pr}(x) = 1 - Y_f(x) \tag{4.19}$$

while in the outer region

$$Y_{pr}(x) = 1 - Y_{ox}(x) \tag{4.20}$$

where $Y_{ox}(r \to \infty) = 1$.

4.3 DNS' Numerical Solution

As mentioned in the previous subsection, the DNS of a turbulet reacting jet requires several computational resurces to solve istantaneously the Nevier-Stokes equations.
The implementation of algorithms, which will optimize the huge calculations required, is as much important as critical; there are different optimization strategies and the most important is the parallel computing approach.
In a parallel computing approach, multiple processor are used together with the aim to distribute the computational cost and reduce the time required

to complete a simulation.
This can be realized using machines with a variety of different structures e.g. Symmetrical multiprocessor(SMP), Massively Parallel Processors (MPP),Single processor and Cluster.
-The SMP consists of two or more identical processors connected to a common main central memory but work independently while the central memory is performed by a dedicated system bus.
-The MPP system consist of a very high number of indipendent processors that are connected together and work as a single computer. In this system there is a single distributed memory which is accessed locally by each single processor so that each processor could be able to acces to its own memory area and code part.
-A single processor which is serial by nature.
-A computer cluster consists of a set of connected computers through fast local area networks; they work togeter computing unit of a cluster runs its own instances.
These systems had better develop through a parallel programming approach to take advantage of their performances.
Many compiler and libraries are aviable to follow this aim like OpenMP and MPI directives which have been adopted in the present work in order both to develop the numerical tools required to perform the simulations and to increase the algorithms performance.

4.3.1 Numerical Code

The considered algorithms has been implemented also to perform the direct numerical simulations of sprays and it has been optimized by the parallel programming approach is going to be explained.
The numerical code adopted is based on a pre-existing code achived in the Department of Mechanics and Aeronautics of "La Sapienza" (University of Rome); it's called CYCLON and it has been modified to pursue the thesis' goal.
This code is able to simulate properly reacting turbulent flows both through DNS and LES solving modified Navier-Stokes equations considered in a low Mach number regime; it has been written through the FORTRAN-90 programming language and its structure can be divided into two main part:

Parallel Algorithm for the carrier phase equations The first part of the code is dedicated to the solution of the Navier-Stokes equations considered in a low Mach number expansion.It is based on a fully explicit Runge-Kutta method with a third order of accuracy.
In this part the carrier phase equations, which has been previously adopted and validated in several studies, are solved using the so called projection mehtod.
In addiction it can be observed a decomposition of the domain over which the equations want to be solved in order to make the parallel code be efficient; this task is accomplished through the decomposition of the system of the Navier-Stokes equations in a series of sub-problems joined together by some specific boundary conditions.

Parallel Algorithm for droplets equations The second part of the Cyclon code considers the droplet motion and evaporation equations, it can be considered as a separate numerical code that works indipendently by the main carrier phase module.
The droplet module is written with a parallel approach and so that all droplet's features impremented are executed simultaneously by each process running on each differet sub-domain.
However every single droplet moves through the sub-domains transported by the main carrier phase: in order to evolve each droplet dynamics through the entire fluid field at every time step a subroutine identifies all droplets in the proximiy of each sub-domain and sends their variables to the process running on the neighbouring one in which the droplet is going to enter.This is possible thanks to MPI directives.
This procedure which is accomplished simultaneously by all runing process, leads to a significant reducion of computational costs.

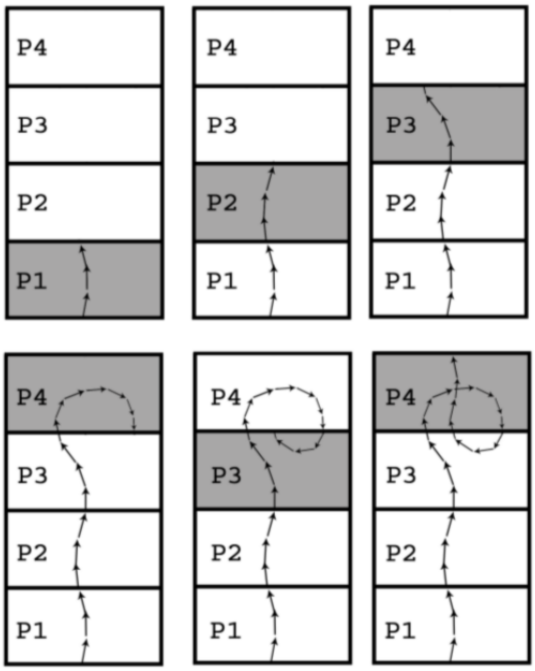

Figure 4.2: The figure shows the area that identifies the process computing the dynamics of a single particle moving across the sub-domains at the rispective time step.

4.3.2 Low Mach Number Equations

In order to derive the Navier-Stokes equations for a reactive turbulent flow in a field caracterized by a low mach number it is convenient to convert the mass conservation and state equations to a non dimensional form.
To this purpose some carries phase variable, evaluated on the jet inlet section, are taken as reference values: ϱ_∞, p_∞, u_{infty}, and r_∞ which are respectively the average density, pressure and volocity and the jet inlet radius.
Also for thermal conducivity, specific heat, binary diffusion coefficient viscosity and specific gas constant are considered reference value: k_∞, $c_{p\infty}$, D_∞, μ_∞, R_∞.
From this reference values it is possible to define the following derived values:

$$t_\infty = \frac{r_\infty}{u_\infty} \quad e_\infty = p_\infty \varrho_\infty \quad h_\infty = \frac{p_\infty}{\varrho_\infty} \quad T_\infty = \frac{p_\infty}{R_\infty \varrho_\infty} \quad f_\infty = \frac{\varrho_\infty u_\infty^2}{r_\infty}$$

which are the reference time, the specific energy, the specific enthalpy, the temperature and force per unit mass which have been used in the non dimensional equations.
In addiction the subsequent non dimensional groups are considered:

$$\tilde{M}a = \frac{u_\infty}{\sqrt{\frac{p_\infty}{\varrho_\infty}}} \quad Sc = \frac{\mu_\infty}{\varrho_\infty D_\infty} \quad Pr = \frac{c_{p\infty}\mu_\infty}{k_\infty}$$

$$Re = \frac{\varrho_\infty u_\infty r_\infty}{\mu_\infty} \quad Ce_i = -\frac{\varrho_\infty \Delta H_i}{p_\infty} \quad Da_i = \frac{\omega_{a\infty}}{\varrho_{infty} t_\infty}$$

where $\tilde{M}a$ is equal to $\sqrt{\gamma}Ma$ where Ma is the Mach number while Sc and Pr are the Schmidt and Prandlt numbers of the carrier phase.
The non-dimensionalization procedure consists in diving each equation for the respective non-dimensinal group leading to the following non dimensional equations:

$$\frac{\partial \varrho}{\partial t} + \nabla \cdot (\varrho \mathbf{u}) = 0 \tag{4.21}$$

$$\frac{\partial}{\partial t}(\varrho \mathbf{u}) + \nabla \cdot (\varrho \mathbf{u}\mathbf{u}) = \frac{1}{Re}\nabla \cdot \tau - \frac{1}{\tilde{M}a}\nabla \cdot p + \mathbf{f} \tag{4.22}$$

$$\frac{\partial \varrho Y_i}{\partial t} + \nabla \cdot (\varrho \mathbf{u} Y_i) = \frac{1}{ReSc_i}\nabla \cdot (\mu \nabla Y_i) + \dot{\omega}_i \tag{4.23}$$

$$\frac{\partial}{\partial t}(\varrho e_t) + \nabla \cdot (\varrho \mathbf{u} e_t) + \tilde{Ma}^2\big(\frac{\partial}{\partial t}(\varrho \frac{u^2}{2}) + \nabla \cdot (\varrho \mathbf{u} \frac{u^2}{2})\big) = \frac{Ma^2}{Re}\nabla \cdot (\tau \mathbf{u}) - \nabla \cdot (p\mathbf{u}) + \\ + \tilde{Ma}^2 \mathbf{uf} + \frac{\gamma}{\gamma+1}\frac{1}{RePr}\nabla \cdot (k\nabla T) + \frac{\gamma}{\gamma-1}\sum_i \dot{\omega}_{\Delta H} \tag{4.24}$$

$$p = \varrho(1 + WY_{iv})T \tag{4.25}$$

The parameter W appearing in the gas state equation is defined as a function of the ratio between the molecular weight of gas and vapour: $\frac{M_g}{M_v} - 1$.
Now it is necessary to express each variable as the following asymptotic series:

$$f(x,t) = f_0(x,t) + f_1(x,t)\tilde{Ma} + f_2(x,t)\tilde{Ma}^2 + f_3(x,t)\tilde{Ma}^3 + O(\tilde{Ma}^3) \tag{4.26}$$

Applying the series expansion to the Navier-stoker equations(the full procedure will be omitted) and gathering together the same order terms it can be noted, from the momentum equation, that the zeroh and first order terms of thermodynamic pressure are uniform over the fluid domain while the second order term in, in general, non uniform.
For this reason the internal energy of the two first orders is constant(it is proportional to $p(t)$),and it can be write:

$$\tilde{f_0} = f_0 + f_1\tilde{Ma}$$

$$f = \tilde{f_0} + f_2\tilde{Ma}^2 + \tilde{Ma}^3$$

Going on with this series expansion the procedure leads to the following equations that are basic for reactive flows in a low Mach number regime.

$$\frac{\partial \varrho_0}{\partial t} + \nabla \cdot (\varrho \mathbf{u})_0 = 0 \tag{4.27}$$

$$\frac{\partial}{\partial t}(\varrho \mathbf{u})_0 + \nabla \cdot (\varrho \mathbf{u}\mathbf{u})_0 = \frac{1}{Re}\nabla \cdot \tau_0 - \nabla \cdot p_2 + \mathbf{f_0} \tag{4.28}$$

$$\frac{\partial}{\partial t}(\varrho Y_i)_0 + \nabla \cdot (\varrho \mathbf{u} Y_i)_0 = \frac{1}{ReSc_i}\nabla \cdot (\mu \nabla Y_i)_0 + Da_i \dot{\omega}_{i0} \tag{4.29}$$

$$\frac{\partial}{\partial t}(\varrho e_t)_0 + \nabla \cdot (\varrho \mathbf{u} e_t)_0 = \frac{\gamma}{\gamma - 1}\frac{1}{RePr}\nabla \cdot (k \nabla T)_0 + \frac{\gamma}{\gamma - 1}\sum_i Da_i \dot{\omega}_{\Delta H} \tag{4.30}$$

$$p = \varrho(1 + WY_i)T \tag{4.31}$$

4.4 Conservation Equations for Turbulent Reacting Flows

The Navier-Stokes equations for turbulent reacting flows are going to be explained considering the coupled evaporating terms and then highlighting the terms associated to combustion.

Conservation of Mass The equation of mass conservation is the same both for reacting and non reactiong flows.

$$\frac{\partial \varrho}{\partial t} + \nabla \cdot (\varrho \mathbf{u}) = 0 \tag{4.32}$$

Conservation of Momentum The equation of momentum for a multi-species mixture, is the same both in reacting and in non reacting flows:

$$\frac{\partial}{\partial t}(\varrho \mathbf{u}) + \nabla \cdot (\varrho \mathbf{u}\mathbf{u}) = \nabla \cdot \tau - \nabla \cdot p + \mathbf{f} \tag{4.33}$$

where f is the volume force.This equation doesn't include any explicit reaction term even if the combustion modifies the flow indirectly: in fact the dynamic viscosity change due to the temperature variation.

For the same reason also density changes, as a conseguence, dilatation occurs and the flame front increases its speed: the local Reynolds number varies much more that in a non-reacting flow and even though the momentum equation is the same, the flow behaviour is different.

Conservation of Species The mass conservation for species i can be write:

$$\frac{\partial \varrho Y_i}{\partial t} + \nabla \cdot (\varrho \mathbf{u} Y_i) = \nabla \cdot (\varrho D \nabla Y_i) + \dot{\omega}_i \tag{4.34}$$

where D is the binary diffusin coefficient of the vapuor of the species and $\dot{\omega}_i$ is the reaction rate of the species i.
As previously seen, considering the all species of the mixture, the total mass conservation is unchanged compared to non reacting flows; in fact combustion does not generate mass, it can be deduced summing on every species $\sum_{i=1}^{Ns} Y_i = 1$ and considering $\sum_{i=1}^{Ns} \dot{omega}_i$.
It can be observed that there are $Ns + 1$ equations to solve describing the mass conservation but only Ns are indipendent; the simpliest method to deal with this problem is to solve the global mass conseration considering $Ns - 1$ mass equations and to make the last species mass fraction adsorb all inconsistences introduced by the other species.

$$Y_{Ns} = 1 - \sum_{i=1}^{Ns-1} Y_i \tag{4.35}$$

Usually the last species is a diluent such us N_2 in this case; however it's important to underline that this semplification should be used only when flames are stronghly diluted (e.g. in air).

Conservation of Energy The energy conservation equation ban be seen as an application of the first law of thermodynamics.

$$\frac{\partial}{\partial t}(\varrho e_t) + \nabla \cdot (\varrho \mathbf{u} e_t) = \nabla \cdot (\tau \mathbf{u}) - \nabla \cdot (p\mathbf{u}) + \mathbf{uf} + \nabla(k \nabla T) + \dot{\omega}_{\Delta H} \tag{4.36}$$

The total specific energy of the carrier phase is e_t while k is the termal conducivity and $\dot{omega}_{\Delta H}$ is the heat source term.

State Equation At last this equation relates the state variables of a thermodynamic system under the assumption that the mixture behaves as a perfect gas.

$$p = \varrho\big((1 - Y_{iv})R_g + Y_{iv}R_v\big)T \tag{4.37}$$

4.4.1 Reaction Rates' Calculation

In the present thesis the existent code Cyclon has been implemented developing the combustion studied for N-species and M-reactions.
A new module has been created, it allows to read the data of the species and reactions in input and then to calculate the reaction rate for each species, the heat source rate and, as a consequence, the heat realeased by combustion that directly influences the solution of the Navier-Stokes equations.
At first the reaction rate $\dot{\omega}_m$ must be calculated, its calculation is based, as disclose in section 2.3, to the Arrhenius law:

$$\dot{\omega}_m = k_m T^{\beta} e^{\frac{-Ea_m}{RT}} \sum_i (Y_i)^{a_{m,i}} \tag{4.38}$$

The value of the pre-exponential factor k, the exponent β and the activation energy Ea are funcion of the raction, while the exponent a changes both for the single species and the reaction.
Subsequently this reaction rate has been used to calculate the reaction rate of each species and the heat source rate:

$$\dot{\omega}_i = \sum_m \dot{\omega}_m \nu_{m,i} \tag{4.39}$$

$$\dot{\omega}_{\Delta H} = \sum_m \dot{\omega}_m \Delta H_m \tag{4.40}$$

where ν is the stoichiometric coefficient of the i-species for the m-reaction while ΔH is the combustion enthalpy of the m-reaction.
However in the present work, it has been considered a global reaction in which the heptane(fuel) reacts with the oxigen(oxidizer) in the following way:

$$C_7H_{16} + 11O_2 \longrightarrow 7CO_2 + 8H_2O \tag{4.41}$$

In order to calculate the rates that are previously threated it has been necessary to found some values, in fact k,Ea,a,β,ν,ΔH are input data.
While the stoichiometric coefficients are known from the global reaction espression and, though the knowledge of them and the formation enthalpy of the species, it is possible to calculate ΔH_m; k,Ea,a,β have been choosen according to Westbrook and Dryer: The pre-exponential factor is 5.1 x 10^{11} $cm^3/mols$, the activation energy is 30kcal/mol, the exponent β is 0 and the exponent a is 0.25 for the fuel and 1.5 for the oxidizer.

Chapter 5

Results Analysis

5.0.2 Setting of Reactants and Validation

A further validation of the combustion model have been made semplifying the flame configuration to a zero-dimensional system.
However the zero dimensional system doesn't take into account a non premixed process, so it has been necessary a relation between the reactant's mass fraction and the equivalence ratio in order to set their initialy concentration up.
This relation has been found considering the previous stoichiometric reaction (4.35) and remembering that air contains $80\%N_2$, which is an inert, and $20\%O_2$ so that the ari molar concentration can be expressed by:

$$[X_{air}] = \alpha[X_{O_2}] + (1-\alpha)[X_{N_2}] \tag{5.1}$$

where $\alpha = \frac{20}{100}$; in a molar concentration form it can be written:

$$[X_{C_7H_{16}}] + \frac{11}{\alpha}(\alpha[X_{O_2}] + (1-\alpha)[X_{N_2}]) \longleftarrow 7[X_{CO_2}] + 8[X_{H_2O}] + \frac{1-\alpha}{\alpha}[X_{N_2}] \tag{5.2}$$

han the non dimensional mole fraction for the i^{th} species can be obtained dividing each term of the left side of the chemical equation for the total molar concentration of the reactants.

$$X_{C_7H_{16}} = 1/56 \quad X_{O_2} = 11/56 \quad X_{N_2} = 44/56$$

Recalling the expression of the equivalent ratio, a dependence for the mole fraction on this can be obtained:

$$\Phi = \frac{(\frac{X_{fuel}}{X_{air}})}{(\frac{X_{fuel}}{X_n air})_{st}} \tag{5.3}$$

$$\begin{cases} X_{C_7H_{16}} = \frac{\Phi}{(\phi + \frac{11}{\alpha})} \\ X_{O_2} = (1 - X_{C_7H_{16}})\alpha \end{cases} \tag{5.4}$$

Anyway the code requires the mass fraction Y_i; the relation between mole and mass fraction is easy and needs only the knowlege of the molecular weights of the species.

$$Y_i = \frac{X_i W_i}{\sum_i X_i W_i} \tag{5.5}$$

In the zero dimensional system both reactants and combustion products are supposed to be concentrated in a single point; through this system the accuracy of the combustion model has been tested knowing that, with the assumption that the heat capacity are all equal indipendent, the variation of enthalpy is equal to the variation of the internal energy and verifying the calculation of the reaction rates.
After using the zero dimensional system, other tests have been made in a mono dimensional ones; in the mono dimensional system a planar laminar premixed flame which propagates in one direction has been considered, this case is an idealized ones because it doesn't represent any real combustion event but it is extremely usefull in order to calibrate the thermo-chemical parameters and to understand the behaviour of the reaction.
The one-dimensional problem of a planar laminar premixed flame propagating into premixed gas is the simpliest flame configuration which can be studied; also from the numerical techniques point of view is a fisrt step toward more complex configurations. There are many ways to compute laminar flame structure and speed depending on the complexity of the chemistry but when chemistry is simplified, analytical or semi-analytical solutions may be easily developed.
For a laminar one-dimensional premixed flames, in fact, the conservation equations can be simplified as follows:

- Mass conservation

$$\frac{\partial \varrho}{\partial t} + \frac{\partial \varrho u}{\partial x} = 0 \tag{5.6}$$

- Species conservation

$$\frac{\partial \varrho Y_i}{\partial t} + \frac{\partial}{\partial t}\big(\varrho(u+V_i)Y_i\big) = \dot{\omega}_i \tag{5.7}$$

- Energy

$$\varrho C_p\Big(\frac{\partial T}{\partial t} + u\frac{\partial T}{\partial x} = \dot{\omega}_{\Delta H} + \frac{\partial}{\partial x}\Big(\lambda\frac{\partial T}{\partial x} - \varrho\frac{\partial T}{\partial x}\Big(\sum_{i=1}^{N} C_{p,i}Y_iV_i\Big) \tag{5.8}$$

where V_i is the diffusion velocity of the i species.

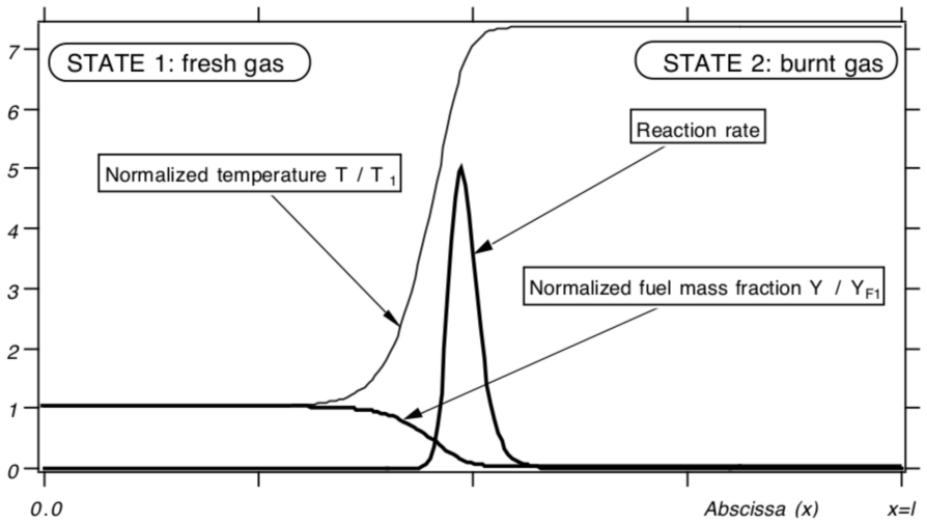

Figure 5.1: Basic configuration for computations of one-dimensional premixed flames

Through the Mono-D system the pre-exponential factor has been calibrated and the flames speed of both a laminar heptane and a laminar n-octane flames have been calulated in order to verify the correctness of the kinetic model according to the procedure described in the work of Westbrook and Dryer [7] who found a relation between the equivalence ratio and the flame speed of an n-octane laminar flame.
Their relation, in fact, can be applied to any type of fuel molecule to develop and validate simplified reaction mechanisms.
The effectuated analysis has shown that the laminar flames speed trend(Fig 5.2) follows the n-octane ones calculated by Westbrook and Dryer even if

when the equivalence ratio grows, for Φ greather than 2, flame speeds calculated in the present work are a bit faster than the n-octane flame of Westbrook and Dryer (until about 5 cm/s at $\phi = 4$).
This difference between the two experiment, probably, is caused by the different estimate of the c_p; in fact, in the present work, it has been considered to be constant.

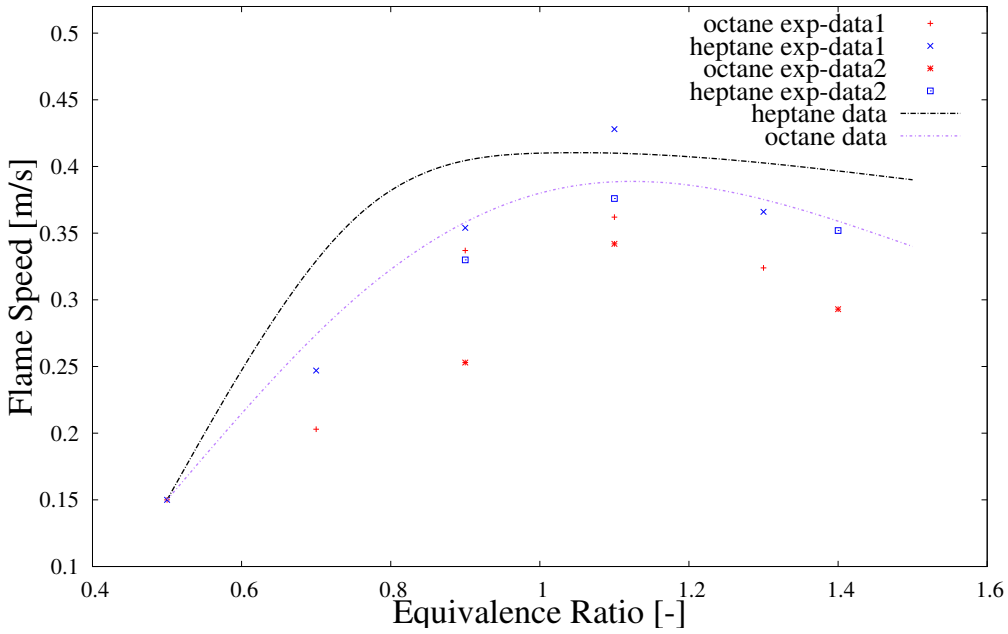

Figure 5.2: Variation of flame speed with equivalence ratio, comparison between the experimental data found by Westbrook and Drayer and the 1D model.

However, it has been decided to reduce the pre-exponential factor, in order to respect the experimental data found by Lipzig, Nilsson, Goey and Konnov. For this reason the pre-exponential factor has been re-calibrate to make the model respect better the experimental data: the found flame speed is about 33 cm/s where $\Phi = 1$.

5.1 Laminar Flames

5.1.1 The Study of Lifted Flames

Lifted flames are found in a lot of pratical applications ad they are of interest since they are simple systems which exibit important characteristics of turbulent-chemistry interaction, finite rate chemistry, heat release and local extinction of combustion. The stabilization characteristic of laminar non-premixed jet flames of pre-vaporized fuel have been studied several times beacuse their semplicity lends them to joint modeling and experimalntal efforts in on-going research to develop predictive code in turbulent combustion. The stability of this flames is a of prime importance in the study of combustion both from theoretical and from pratical device point of view; in particoular, during this work, the attenction has been focused on laminar flames studied experimentally in heated coflow and for different initial conditions like, for example, low or high temperature and different inlet velocity. It has been reproduced an experiment, menaged by Al-Noman Choi and Chung, which has demonstrated that the edge of a stationary lifted flame has a tribrachial flame structure, paying a particoular attention to the autoingnition phenomenon which assumes a central role in most of pratical combustion systems.
It has been considered a coflow burner with a central fuel nozzle; the central nozzle has an internal diameter of 3.76 mm and the fuel is pure n-heptane(99%) vaporized and diluted with nitrogen so that the mass fraction is $X_f = 0.03$.
Both the vaporized fuel and the coflow air are heated until 960K, at this temperature an autoignited flame has formed.
The experiment has been conducted by varying the fuel jet velocity u_0 and it has shown that the lenght of the flame and the liftoff hight increase with the fuel velocity showing a distinct tribrachial edge structure, consisting of lean and rich premixed flame wings, which can be clearly identified with the naked eye, and trailing diffusion flame.
It has been theorized that the coexistence of these tree flames implies that a tribrachial point do exist and it should be located along the stoichiometric contour of the jet; in addiction the edge propagation speed should be dictated by the premixed flame wings.
As a consequence, the stabilization of stationary lifted tribrachial edge flame can be explained based on balance between the propagation speed of tribrachial flame and the local flow velocity along the stoichiometric contour.
The purpose of the present work is to find evidence that the hypotheses previously quoted work through the analysis of the DNS' results.

Several simulations has been carried out to search the configuration that better get closer the experimental data and so a pre-exponential factor with the value of $1 \cdot 10^{11}$ has been choosen (Fig. 5.3).
It is clear the slope that has been found through the simulations doesn't fit

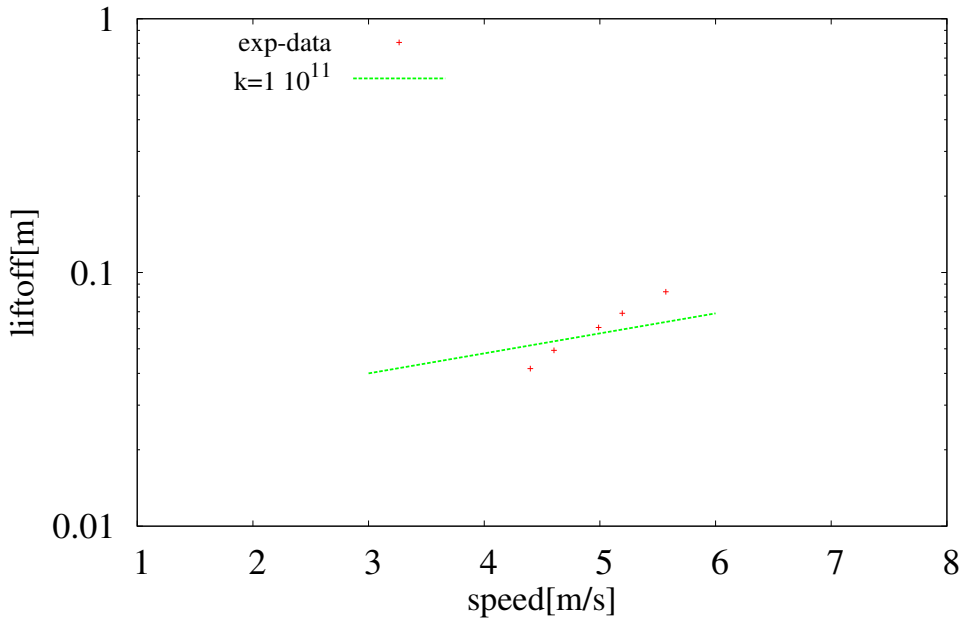

Figure 5.3: Liftoff heights of autoignited flames with fuel jet velocity for a pre-exponential factor of $k = 1 \cdot 10^{11}$ compared with the experimental data.

perfecly the experimental ones, it's probably caused by the significant difference between the approximated global reaction of combustion and the real combustion process.
However the trend can be considered satisfactory and adequate for the analysis of interest.

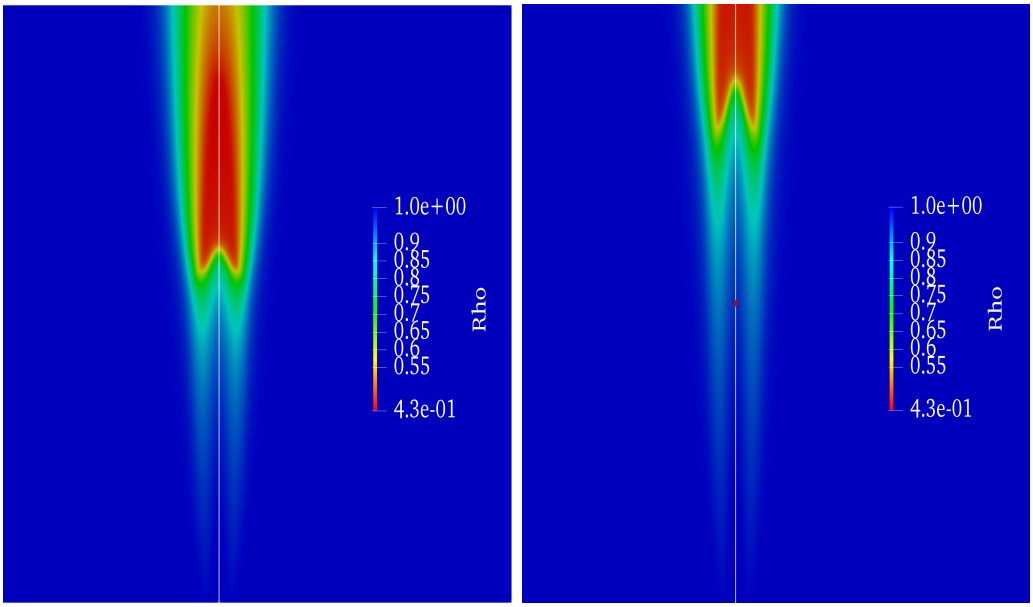

Figure 5.4: Figure shows the variation of the flame lift-height with the fuel inlet velocities for cases $v_{inl} = 3m/s$ and $v_{inl} = 4.6m/s$

5.1.2 Stabilization of the Leading Edge

It has been decided to prove if the implemented model allows to verify the theory which affirm that the propagation speed of the flame is equal and opposit to the flow velocity along the stoichiometric contour at the point where the leading edge occurs.
To do that, it has been reproduced the bi-dimensional simulation with an inlet velocity of 3m/s through the mono-dimensional system finding a laminar adimensional burning velocity of 1.67 to compare with the 2D adimensional velocity along the stoichiometric line in the z-direction at the leading edge.
The stoichiometric line can be easily observe in the Figure 5.6 which rapresent the heptane, the density and the products distrubutions; in this figure it can be noted a rich distribution of the fuel on the internal side of the flame while, on the external side, due to the diffusion and the combustion, the flame is evidently lean.

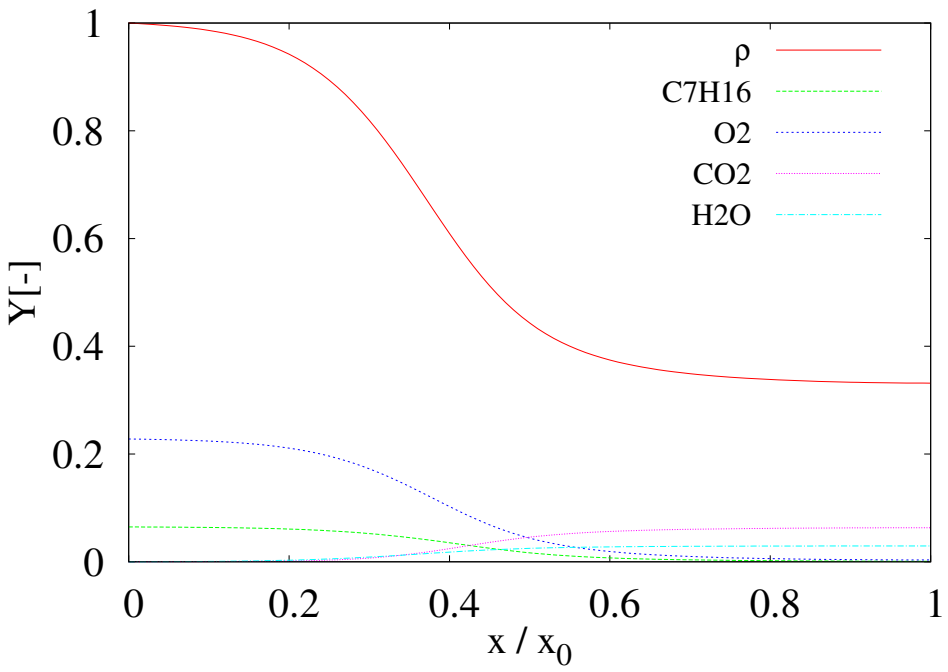

Figure 5.5: Adimensional density and concentrations of fuel, oxidizer and product obtained by reproducing the 2D case with an inlet velocity of 3 m/s on the mono-dimensional sistem

The leading edge is considered to be formed in the region separating the combustive and the combustion products; in fact the flame front is defined as the region of space where the combustion reaction takes place.
Considering the products distribution it can be said that the leading edge has formed at about 22 radiuses (41.4mm) form the nozzle, at this point it can be measured a comparable adimensional velocity of about 1.8 (Fig 5.7); For this reason the hypithesis that has been quoted on the leading edge stabilization can be supposed to be appropriate.

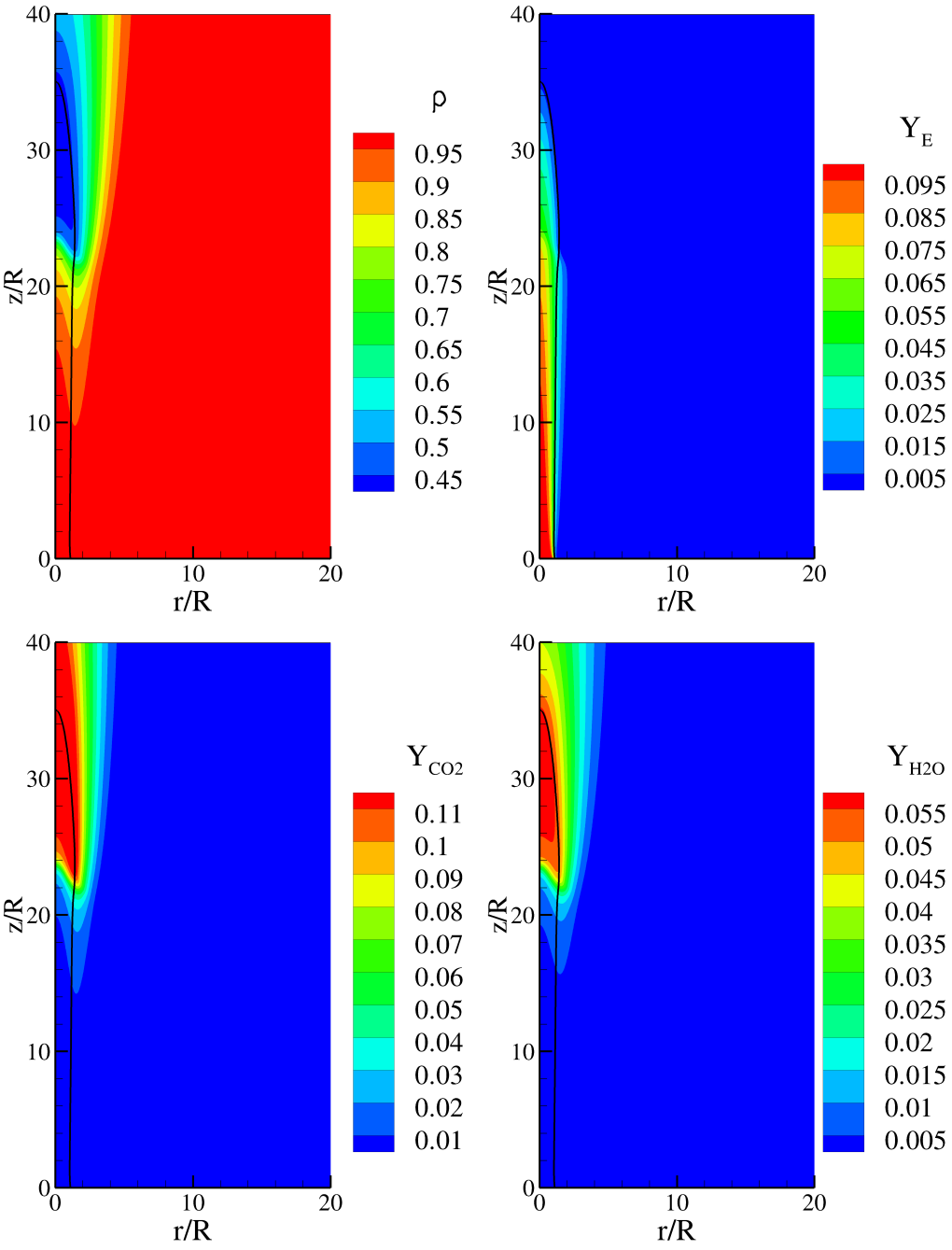

Figure 5.6: 2D data, case $v_{inlet} = 3\text{m/s}$, distributions of density, heptane, CO_2 and H_2O with the stoichiometric contur highlighted by way of black line

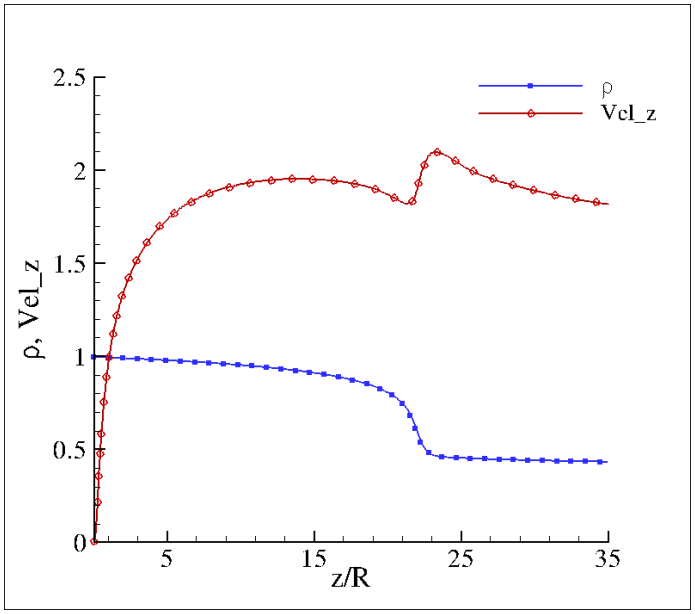

Figure 5.7: Propagation flame speed and density on the stoichiometric contour of the 2D laminar case $v_{inl} = 3m/s$

5.1.3 Combustion Regimes

In addiction a combustion analysis has been realized in order to understand how the flame really burns and the perentage of premixed and diffusive combustion has been calculated on the middle fields.
At first, the Flame Index has been analized in order to quantify the contribution of each type of combustion. The flame index that has been take into account has been modified as follows with the aim to point out multiple levels which has been split into 3 ranges: diffusive combustion, premixed combustion and partially premixed combustion).

$$FI = \frac{\nabla Y_f \nabla Y_o}{|\nabla Y_f \nabla Y_o|} \tag{5.9}$$

As previously said, vanishing FI indicates local non-premixed combustion while a a unity flame index indicates local premixed combustion; in particoular, in this work, the combustion has been considered premixed for values of the $FI > 0.33$, partially premixed when $-0.33 < FI < 0.33$ and diffusive for $FI < -0.33$. Than, also the fuel reaction rate has been divided in order to undestrand better how the combustion happens and how the reaction rate is distributed in the three categories.
In Figure 5.8 end 5.9 it can be observed that the point where the leading edge

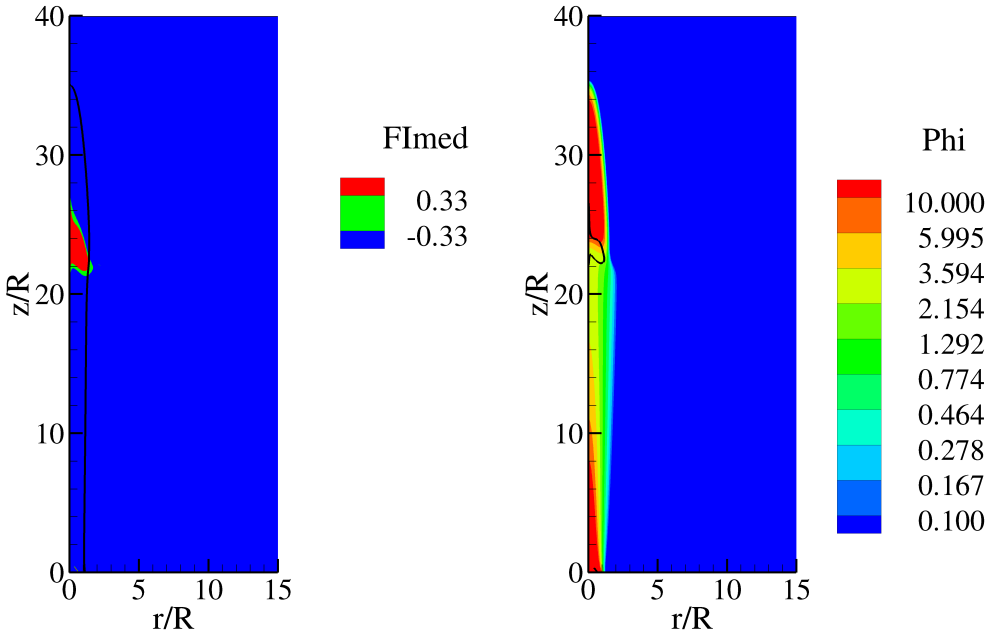

Figure 5.8: Figure shows the flame index with the stoichiometric contur drawn using a black line (left) and the distribution of the equivalent ratio with the isosurface FI=1 highlight using the black line (right)

occurs is characterized by a rich mixture and is a strong premixed point even if the flame evidently starts on the stoichiometric line in a diffusive regime. It can be also observed that, at the bottom, on the inner part of the flame, as teorized, the combustion is totally premixed while the diffusive one which start on the outer part of the leading edge propagates towards the top along the stoichiometric zone.
Between the two type of combustion the third modality happens. This partially premixed combustion occurs on the external side of the stoichiometric contur; it suggest that this type of combustion is realised where the mixture is lean.

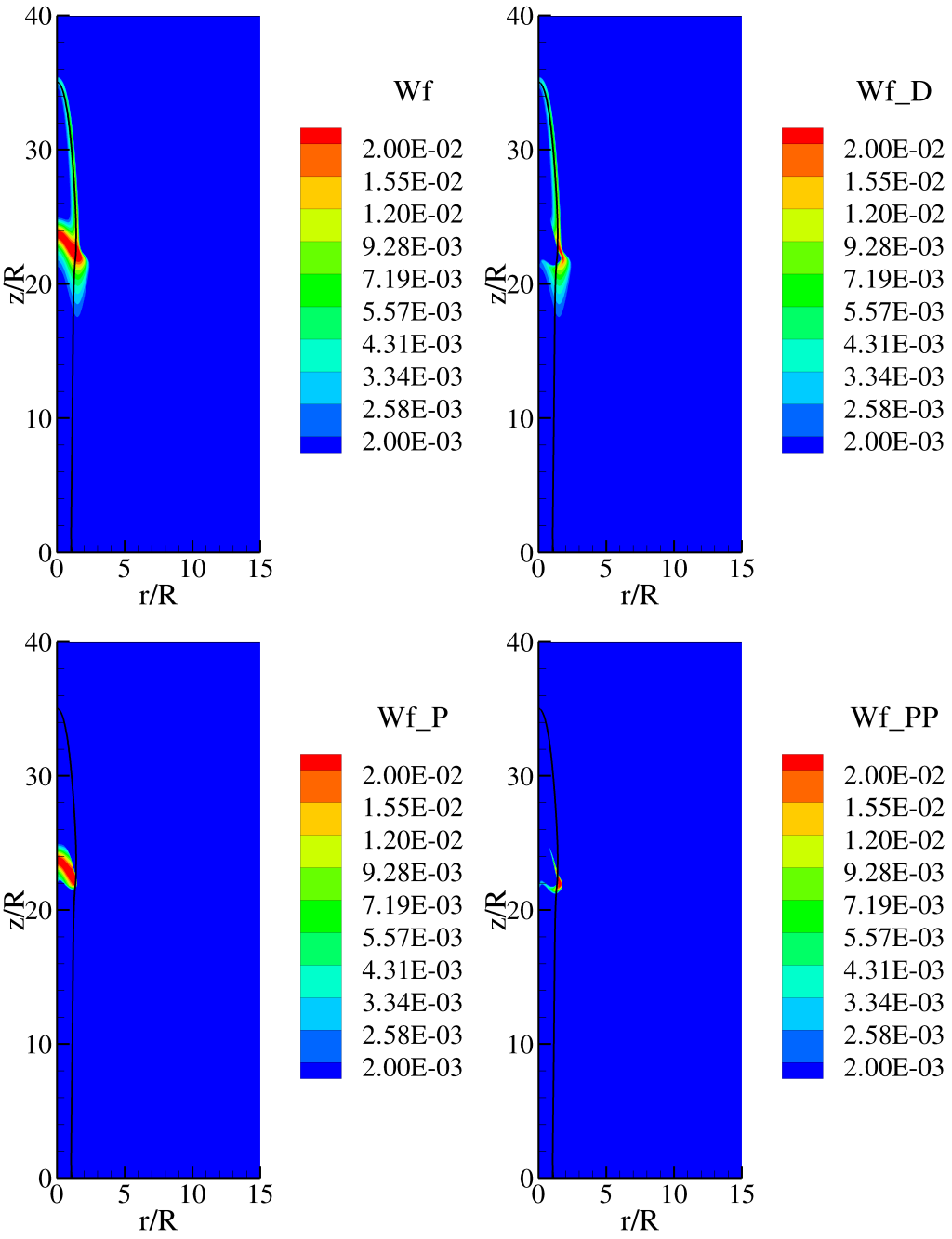

Figure 5.9: Figure shows the mean local reaction rates; It can be observed the global one followed by the diffusive, premixed and partially premixed reaction rate which allow to understand how the flame burns with the middle stoichiometric contur drawn using a black line.

To evaluate the amount of the burning in the various regimes and compare them to the overall heat release rate, there have been introduced the fractions of the burning rate which are only function of the streamwise direction z. The evolutions of the three burning fractions and the overall heat release rate are shown in figure 5.10 where it can be observed that most of the burning occurs in a non-premixed regime included the auto-ignition phenomenon. On the other hand, at the leading edge, premixed combustion is prevalent; it is intresting to note that, when premixed combustion happens, its intensity is greater than the diffusive one even if it is less than this.
However, finally, it can be said that, overall, the percentage of the three regimes of combustion are:
- 70.3% Diffisive combustion,
- 21.22% Premixed combustion,
- 8.46% Partially-premixed combustion.

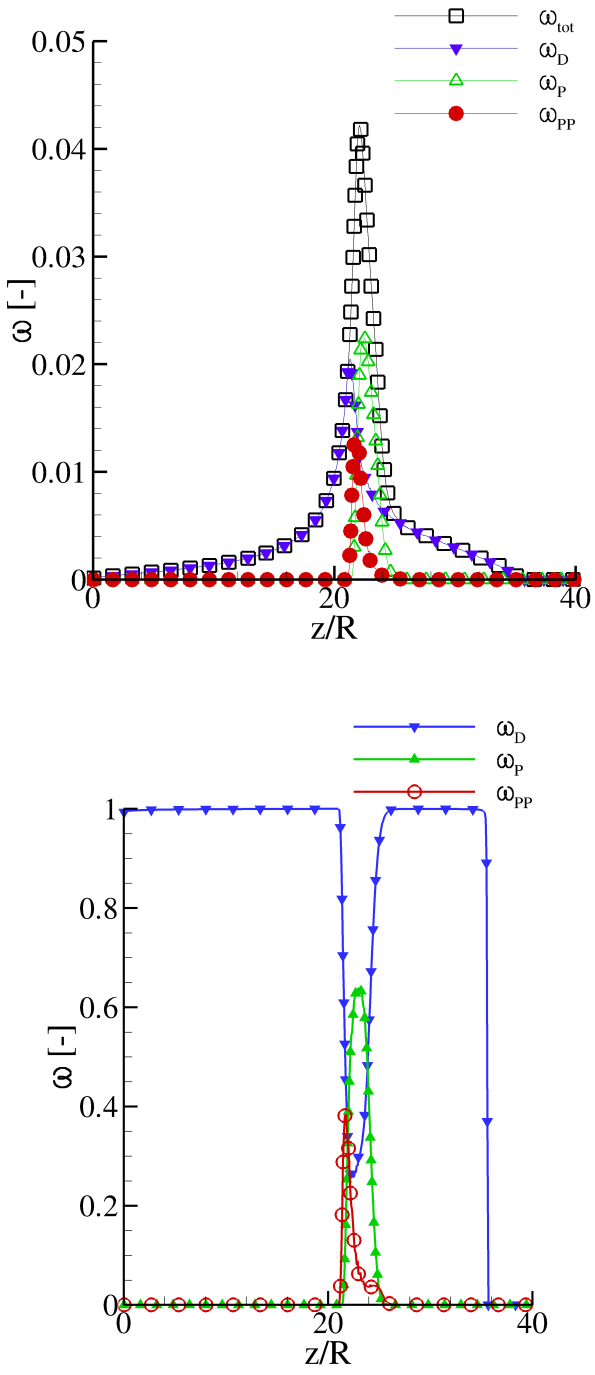

Figure 5.10: Evolutions of the overall heat released, the premixed, partially-premixed and diffusive burning fractions and their probability on the streamwise direction z.

5.2 Turbulent Lifted Flame

The analysis effectuated on the laminar flames have been reproduced on a turbulent flame; it has been decided to layered the pipe diameter and the inlet velocity with the aim to reproduce the same condictions of the laminar case previously analized.
The Reynolds number has been increased to 4000 in order to guarantee a turbulent regime and, as a cosequence, it has been considered an inlet velocity of 10 m/s and a pipe diameter of 22 mm.

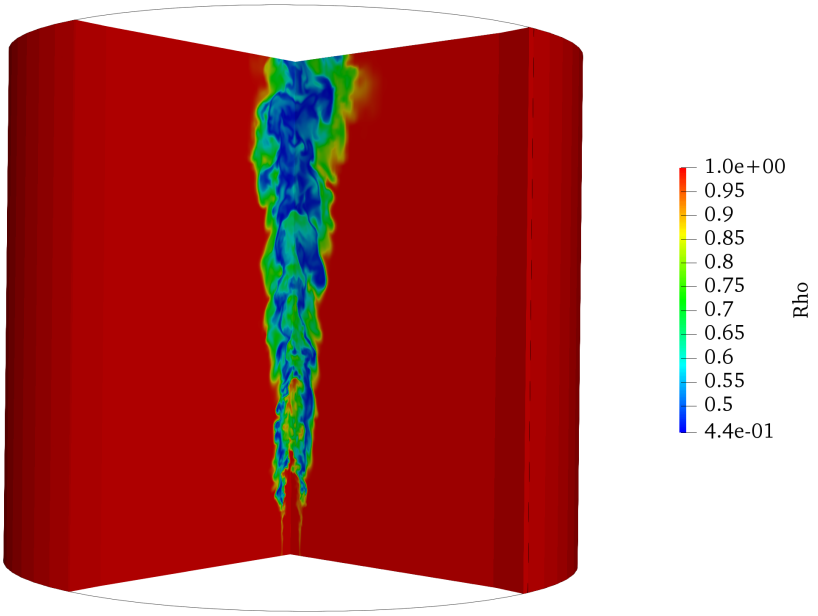

Figure 5.11: Qualitative image of the 3D turbulent flame, istantaneous field.

With the aim to establish the height at which the leading edge occurs, middle fields have been considered; it has been observed that the leading edge occurs at about 88mm and studying the adimensional laminar burning velocity detected at this point, on the stoichiometric contur, it has been noted that it is about three times the burning velocity of the laminar case as experimentally found by Lyons[16].

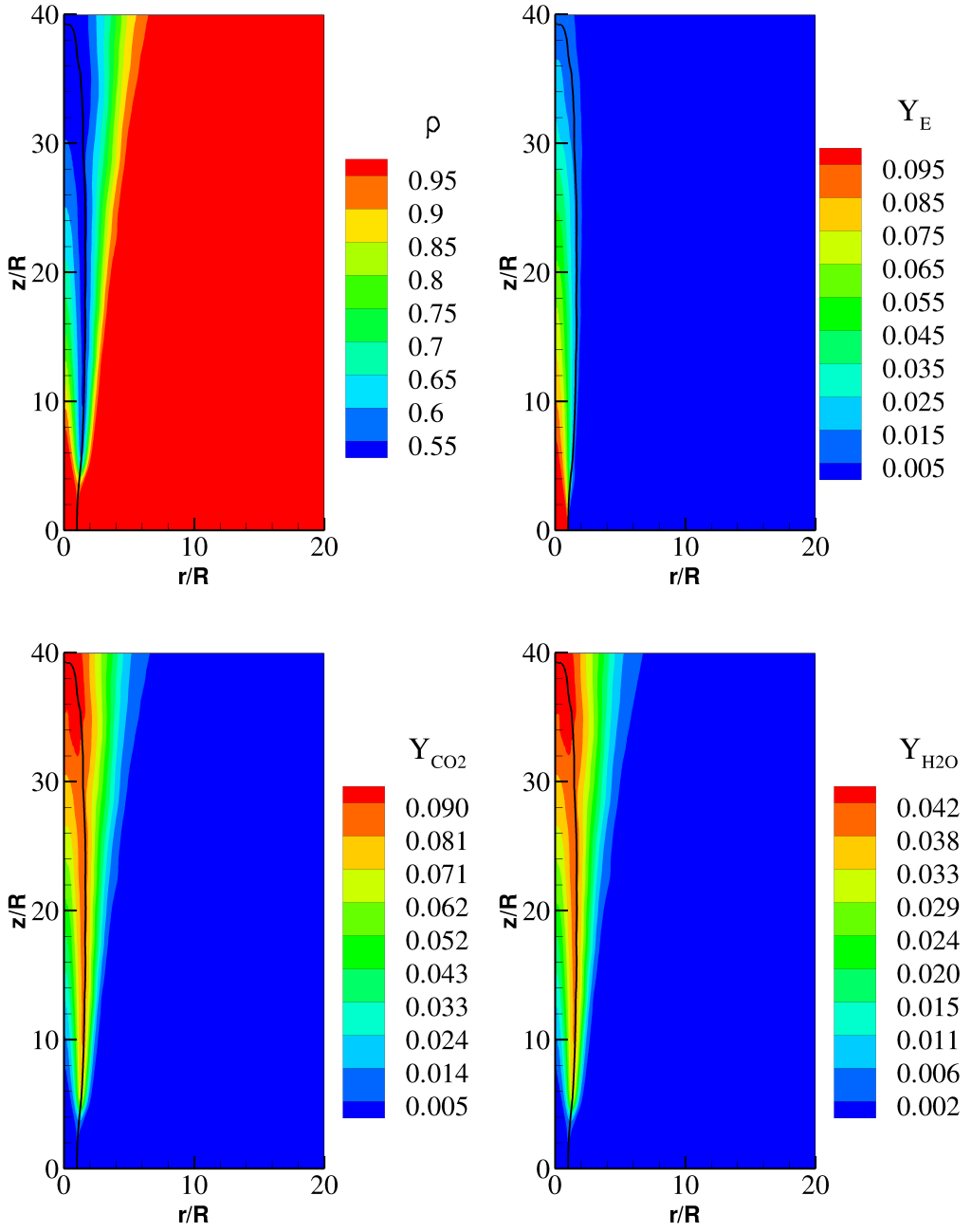

Figure 5.12: Figure shows the mean distributions of density, heptane, CO_2 and H_2O with the stoichiometric contur highlighted by way of black line

However it is important to say that, if istantaneous fileds are considered, it can be observed that the leading edge appears floating and asymmetrical; in fact the leading edge is supposed to be made up of multiple, small fragments of flame rather than a continuous reaction zone. These findings have implications for planar imaging related to the possibility that the true leading edge of the flame is located out of the considered plane.
The structure of the flame has also been analyzed using the flame index; it has already been said that the flame is a premixed flame when the FI is positive and a diffusion flame when it is negative approximately. Fig 5.13 shows the various isosurfaces of the FI on left and the two foundamental considered ranges on the right. The flame index has also been studied on the istantaneous field(Fig.5.14) where a complicated structure is observed n the first image on the left while on the right it is shown the istantaneous equivalent ratio distrubution which make it clear that the most of the flame burns through a rich mixture; It can be noted that from the leading edge, on the inner side of lifted flame, a kind of conical premixed flame surrounded from a diffusion flame is formed.

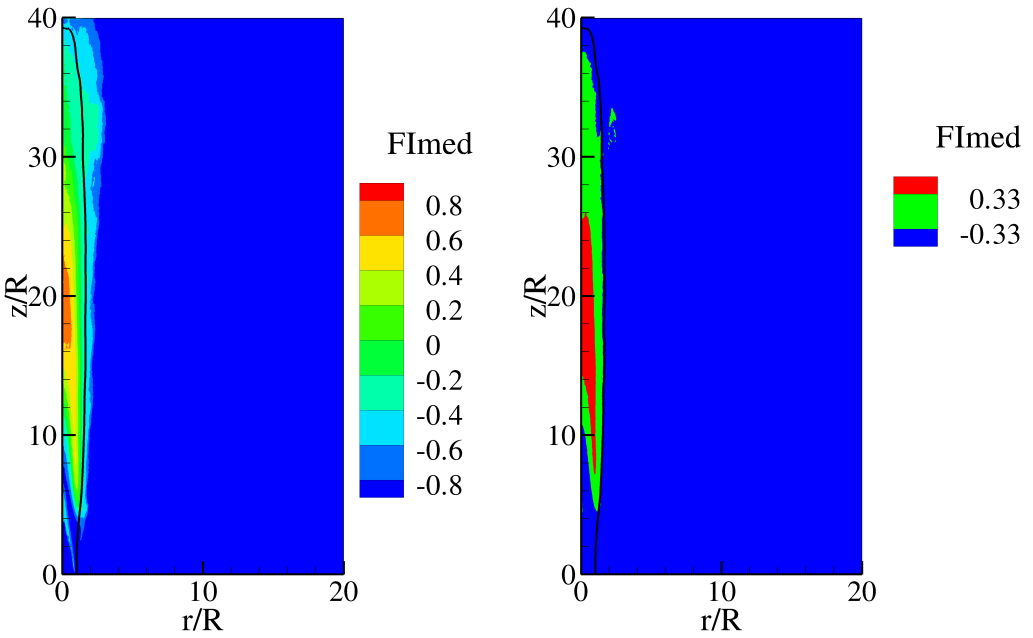

Figure 5.13: Figure shows the mean flame index

In addiction it can be obseved through the close up view around the leading edge that the combustion starts in a premixed regime on the stoichiometric

contur and become a diffusion flame going on toward the top on the stoichiometric line while the premixed flame continues inward forming the conical rich premixed flame.

Also comparing figure 5.12 and figure 5.15 it can be easily seen that while the inner premixed flame is rich, the outer diffusion flame is predominantly aligned along the stoichiometric line or lean.

This confirm one again the triple structure of the flame at the leading edge composed of a rich premixed flame, a diffusion flame and a lean partially-premixed flame and it can be seen more clearly in figure 5.13 where the mean reaction rates are shown; it can be said that the leading edge is stabilized from a sequence of premixed and partially premixed propagation which evolves into a diffusion flame structure going upstream to counter the local flowfield while also modifying it through heat release.

On the stoichiometric contur can also be observed the heigher consumption of the overall reaction rate that is easily seen considering an istantaneous field shown in figure 5.16.

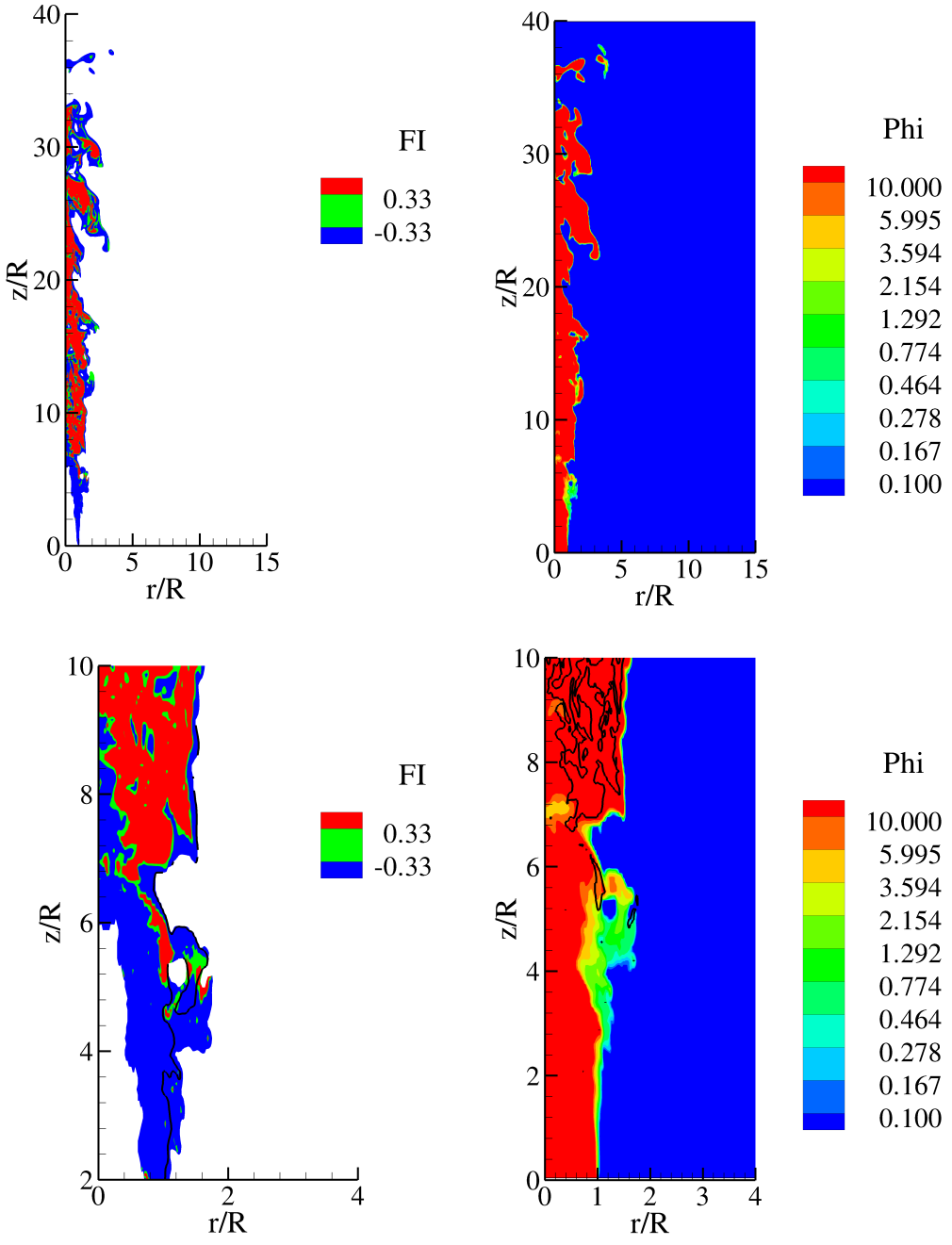

Figure 5.14: Figure shows: on the top the istantaneous flame index (left) and the istantaneous distribution of the equivalent ratio (right); on the bottom a blow-up of the leading edge:on the left the flame index with the stoichiometrc contur drawn using a black line and on the right the equivalent ratio with the isosurface $FI = 1$ hightlight with a black line.

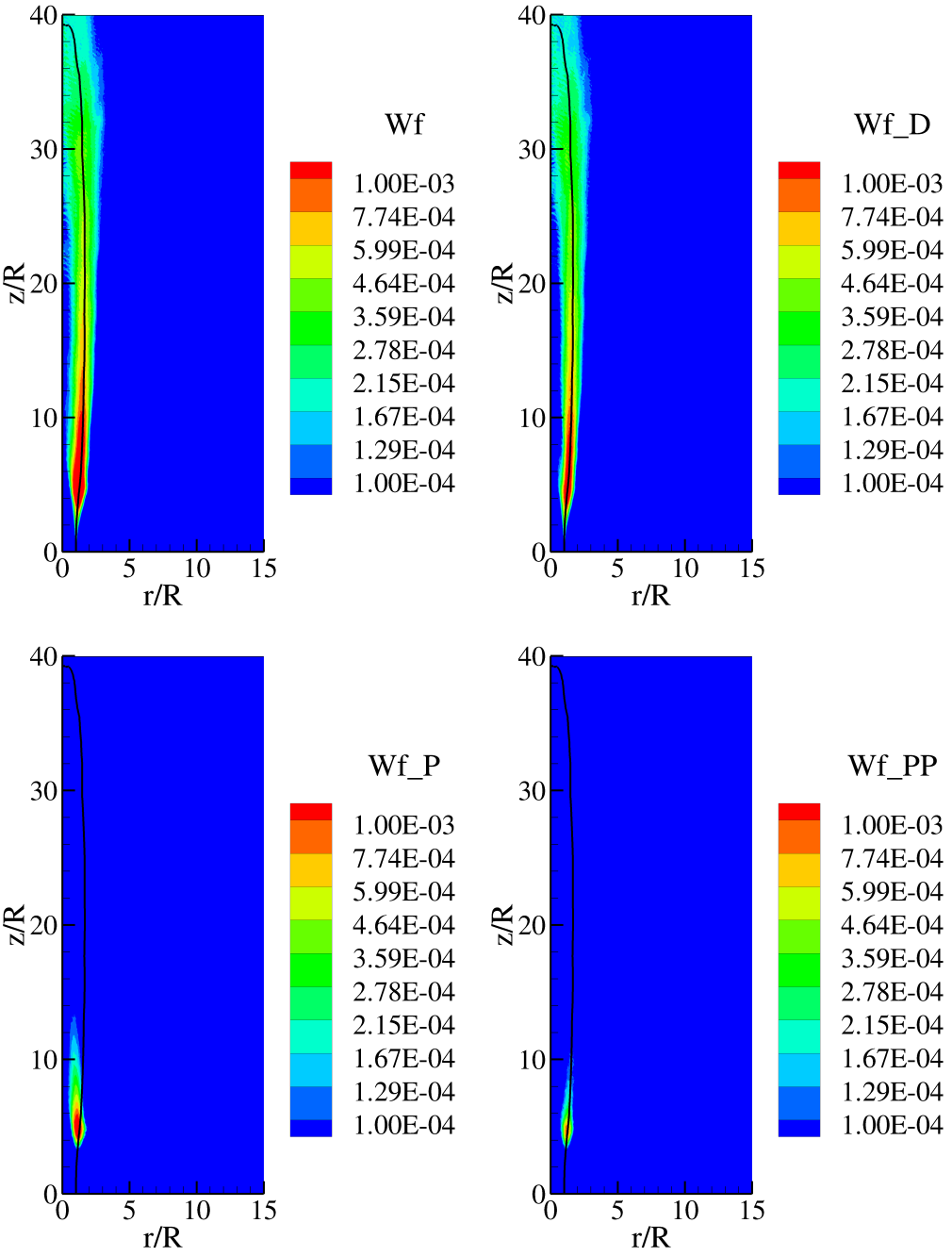

Figure 5.15: Figure shows the mean local reaction rates: the over all reaction rate, the diffusive, premixed and partially premixed one expressed using the same range so that they can be compared.

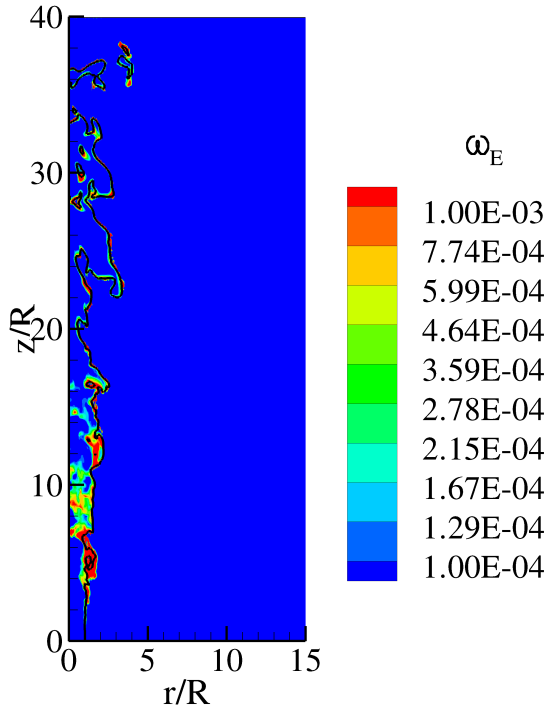

Figure 5.16: Overall reaction rate considered on an istantaneous filed with the stoichiometric contur drawn using a black line

As observed for the laminar case, despite the most of the combustion occurs in a non premixed regime(80.56%), the intensity of the premixed combustion is greater than the other regimes and it is prevalent at the leading edge.
However, unlike the laminar case, in the turbulent lifted flames premixed and partially premixed combustions can be found also throughout the flame thanks to the mixing of the fuel vapor and the surronding air in stoichimetric proportions due to the turbulence, even if their presence and percentage outside the leading edge are even more minimal compared to the diffusive one. In fact the premixed combustion affects the overall combustion for a value of 10.35% while the partially premixed for 9.08%.

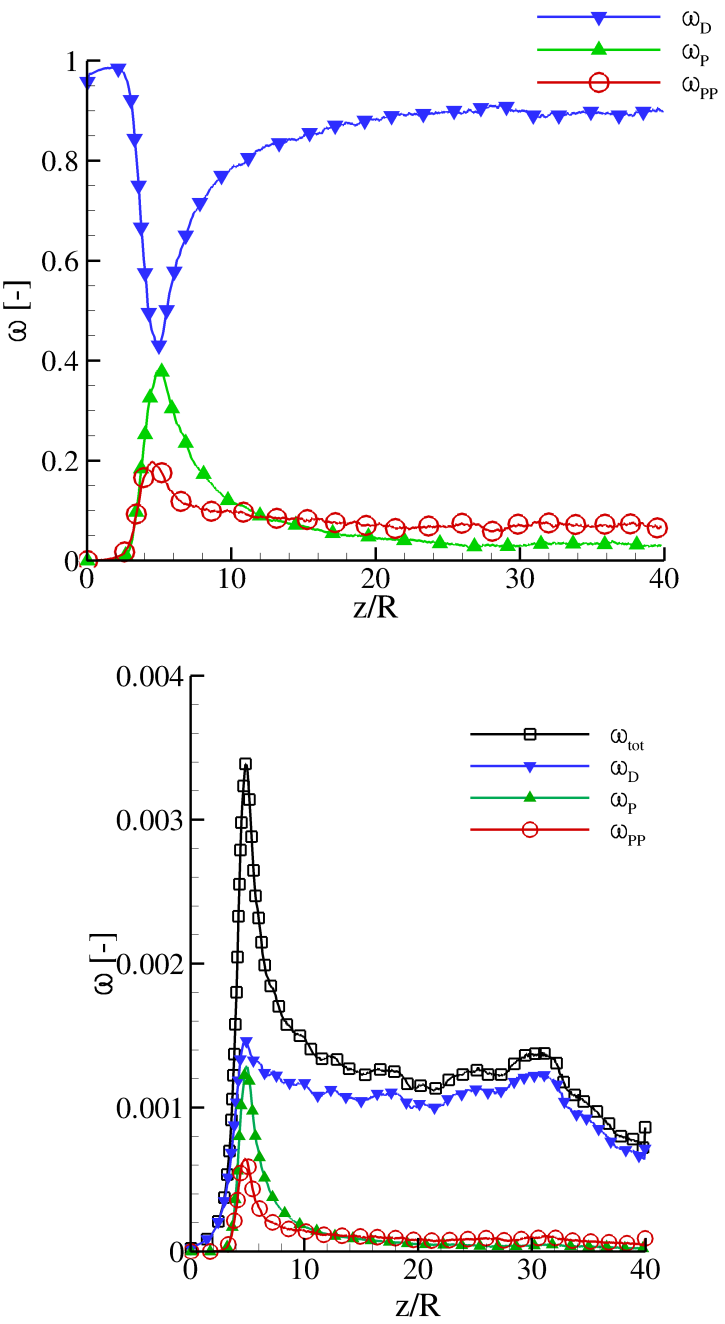

Figure 5.17: Mean local reaction rates integrated along the z direction and plotted as a function of the downstream location; in the first figure it can be seen the probability of each reaction rate while in the second figure the amount of each type of specific reactions rate compared with the global one can be observed.

Chapter 6

Conclusion Remarks

The main achievement of the present work has consisted in the implementation of a module for the chemical kinetics of heptane/air in an existing numerical code named CYCLON. A well known global combustion scheme has been integrated into the CYCLON code which was already able to solve the Navier-Stokes equations for multiphase turbulent flow, e.g. DNS of turbulent sprays.
A former validation process has been realized on the modified code including the global combustion scheme through the comparison between experimental results and numerically computed data using, at first, a mono-dimensional system and than a bi-dimensional one. It has been demonstrated that numerically computed data fit well the experimental results.
The validated code has been adopted to perform a DNS of both laminar and turbulent reacting jets of heptane vapor in air coflow similarly to the experiments of [7] on laminar lifted flames. The analysis of the DNS data has been performed looking both at instantaneous and averaged field and has further demonstrated the capabilities of this numerical code to reproduce the jet burning dynamics. According to experimental evidences, DNS data show that a lifted auto-ignited diffusive flame is stabilized because of a local premixed flame. This structure is called tribrachial flame and can stabilize the flame when the flow velocity can be balanced by the premixed flame speed. However if the equilibrium cannot be attained the flame cannot stabilize and the flame quenches.
The behavior of the laminar regime of the tribrachial flame is compared with the turbulent one. The turbulent flame is stable at much higher jet speed. Even in this case the flame anchoring is provided by a local premixed flame, but in the turbulent regime.
The amount of heat release occurring in premixed and non-premixed regimes has been precisely characterized using the Flame Index indicator. From a

global point of view, the large part of the flame occurs in the non-premixed regime (80% in the laminar and 90% in the turbulent), but the premixed flame dynamics is crucial for a stable flame anchoring.
This findings are important for modeling purposes since usual combustion models are essentially different between these regimes.
In the future DNSs of turbulent reacting evaporating spray of heptane could be performed and studied in order to assess how different are the dynamics when the same fuel is injected in the liquid state.

Bibliography

[1] Chung K. Law *Combustion Physics*, 2006

[2] Stephen B.Pope *Turbulent Flows*, 2001

[3] Stephen R.Turn *An Introduction to Combustion*, 2000

[4] H.Wang, K.Luo, J.Fan *Effects of turbulent intensity and droplet diameter on spray combstion using direct numeical simulation*, Fuel 121:311-318, 2014

[5] W.P.Jones and R.P.Lindstedt *Global Reaction Schemes for Hydrocarbon Combustion*, Conbustion and Flame 73:233-249, 1988

[6] D.Veynante, L.Vervisch *Turbulent combustion modeling*, Progress in Energy ad Combustion Science 28:193-266, 2002

[7] Charles K.Westbrook, Frederick L.Dryer *Simplified Reaction Mechanisms fot the Oxidation of Hydrocabon Fuel in Flames*, Combustion Science and Tecnology 27:31-43, 1981

[8] A.R.Masri *Turbulent Combustion of Sprays: From Diluite to Dense*, Combustion and Science 188(10):1619-1639, 2016

[9] J.Reveillon, L.Vervisch *Analysis of weakly turbulent dilute-spray flames and spray combustion regimes*, Journal of Fluid Mechanics 537:317-47, 2005

[10] G.Borghesi,E.Mastorakos,RS.Cant *Complex chemistry DNS of n-heptane spray autoignition at high pressure and intermediate temperature conditions*, Combustion and Flame 160:1254–75, 2013

[11] J.Seo, KY.Huh *Lagrangian conditional statistics of turbulent n-heptane spray combustion in different injection conditions*, Proceding of the Combustion Institute 34:1687–95, 2013.

[12] Sang Kyu Choi, Suk Ho Chung *Autoignited and non-autoignited lifted flames of pre-vaporized n-heptane in coflow jets at elevated temperatures*, Combustion and Flame 160:1717-1724, 2013.

[13] J.P.J. van Lipzig, E.J.K. Nilsson, L.P.H. de Goey, A.A. Konnov *Laminar burning velocities of n-heptane, iso-octane, ethanol and their binary and ternary mixtures*, Fuel 90:2773-2781, 2011.

[14] S.M. Al-Noman, S.K. Choi, S.H. Chung *Autoignition characteristics of laminar lifted flames of pre-vaporized iso-octane in heated coflow air*, Fuel 162:171-178, 2015.

[15] K.M. Lyons *Toward an understanding of the stabilization mechanisms of lifted turbulent jet flames: Experiments*, Progerss in Energy and Combustion Science 33:211-231, 2007.